Ph.D. DISSERTATION

# IN VITRO DRUG SCREENING BIOCHIP FOR PERSONALIZED CANCER PATIENT CARE

환자맞춤형 치료를 위한

체외 항암제 스크리닝용 바이오칩

AUGUST 2020

SEOUL NATIONAL UNIVERSITY

DEPARTMENT OF ELECTRICAL AND COMPUTER ENGINEERING

SU DEOK KIM

# In vitro drug screening biochip for personalized cancer patient care

# 환자맞춤형 치료를 위한 체외 항암제 스크리닝용 바이오칩

지도 교수 권 성 훈

이 논문을 공학박사 학위논문으로 제출함

2020 년 6 월

서울대학교 대학원

전기정보공학부

김 수 덕

김서 덕의 공학박사 학위논문을 인준함

2020 년 6 월

위 원 장 전 누 리 (인)

부위원장 권 성 훈 (인)

위 원 박 욱 (인)

위 원 김 지 윤 (인)

위 원 최 정 일 (인)

# Abstract

# In vitro drug screening biochip for personalized cancer patients care

Sudeok Kim

Electrical and Computer engineering

Graduate School

Seoul National University

Precision or Personalized Medicine is a medical paradigm aimed to determine optimal therapy for individual patient. In particular, clinical oncology has been using methods of molecular profiling for each patient through next-generation sequencing (NGS), mRNA-sequencing, and mass spectrometry, and has been trying to implement personalized treatment. However, personalized treatment based on molecular profiling to each patient is not always possible due to the high level of heterogeneity of tumor that is still not fully understood at the current level and

acquired resistance of anti-cancer drug due to cumulative targeted therapy. In such cases, in vitro drug testing platform using primary cells obtained from patients, or patient-derived cells, spheroids, and organoids can make it possible to find a more appropriate treatment for each individual patient. However, though high-throughput drug screening technology for this purpose is of the utmost importance in saving lives, there were many limitations to its wide use in many hospitals. The existing high-throughput drug combination screening technology consumes a large number of samples and consumes a considerable amount of expensive reagents. In addition, expensive automated liquid handlers, which were essential for exploring thousands of different pipetting, were not easy to introduce except for large-sized pharmaceutical companies and research institutes, which limited access to technology.

In this study, I construct a heterogeneous drug-loaded microparticle library by fabricating encoded photocurable polymer particle that has individually identifiable codes to track loaded drug. and I load various drug molecules, which I want to test to target cells, into each coded microparticle. Then, I developed to produce heterogeneous drug-laden microparticle arrays through simple self-assembly without the need for a microarray spotter or dispensing machine for generating microarray. I also have developed cell seeding method of seeding small-volume samples into the microwell-based cell chip. By utilizing the drug-laden microparticle

hydrogel array and microwell-based cell chip technology, hundreds to thousands of different assays can be done at once with just a small number of samples and low cost.

Through the implemented platform, the anti-cancer drug sequential combination screening was conducted on the triple-negative breast cooler (TNBC) cells, which are generally known to be difficult to treat due to lack of known drug target, and the results of screening were analyzed by establishing a library of drugs in the EGFR inhibitory type and drugs in the genotoxin type. In addition, another study was conducted to find optimal drug combinations using patient-derived cells derived from tumors in patients with non-small cell lung cancer that have obtained acquired resistance. Finally, as the growing need for three-dimensional culture, such as spheroid and organoid for having a similar response to in vivo drug testing, it was also developed that microwell-based cell chip that is capable of 3D culture with low-cost and small-volume of cells.

The miniaturized in vitro anticancer drug screening platform presented in this study has the following significance. An easy-to-use technique that can be applied to a small number of patient cells or samples, which can dramatically reduce the use of conventional expensive equipment, reagents. The proposed technology in this study can be applied to a variety of academic studies previously inaccessible to high-throughput screening due to the high cost of reagents, the high price of equipment,

or the limited amount of samples in conventional drug screening. and this platform can also dramatically increase access to clinical research in hospitals for personalized treatments. In particular, it is expected that the possibility of this platform will be further maximized if it is used in a relatively small and medium-sized research environment by the combined use of various rare samples such as patient-derived cells or patient-derived organoids.

**Keywords:** precision medicine, microarray, high-throughput screening, drug combination, encoded microparticle, biochip

**Student Number:** 2014-21752

# Contents

**List of Figures**

# Chapter 1 Introduction

In this chapter, I will briefly explain why it is important that high-throughput drug screening using biopsy sample from cancer patient in a small volume is important for saving lives of cancer patients in the era of precision medicine. I will then review previously studied biochip platform utilizing the advantage of miniaturized lab-on-a-chip technology such as using microfluidics approach and microarray-based approaches. Finally, I will present the concept of the miniaturized drug screening platform which utilizes the combinations of polymer technology in drug delivery system and microarray technology is high-throughput bioassay.

## 1.1 Motivation of this research

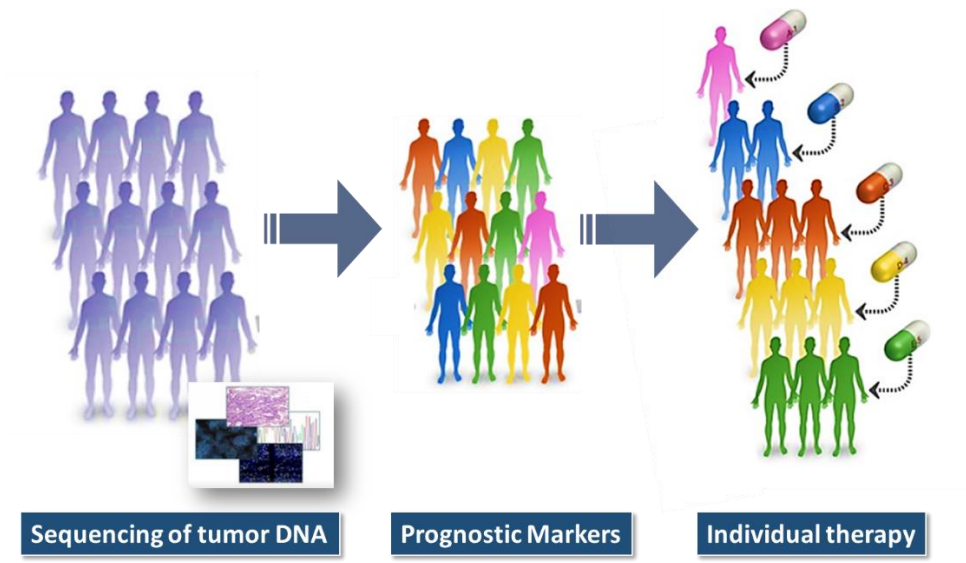


Figure 1.1 The advent of NGS contribute a lot to individualized therapeutic options.

In the era of personalized medicine, personalized cancer therapy is the notion of a treatment strategy centered on the ability to predict which patients are more likely to respond to specific cancer therapies.[1–3] This approach is founded upon the idea that tumor biomarkers are associated with patient prognosis and tumor response to therapy.[3,4] In addition, patient genetic factors can be associated with drug metabolism, drug response and drug toxicity. Personalized tumor molecular profiles, tumor disease site and other patient site and other patient characteristics are then

potentially used for determining optimum individualized therapy options.[1,5] Tumor biomarkers can be DNA, RNA, protein and metabolomic profiles that predict therapy response. However, the most recent approach is the sequencing of tumor DNA by using NGS sequencer. And it can reveal genomic alterations that have implications for cancer treatment. (Figure 1.1)

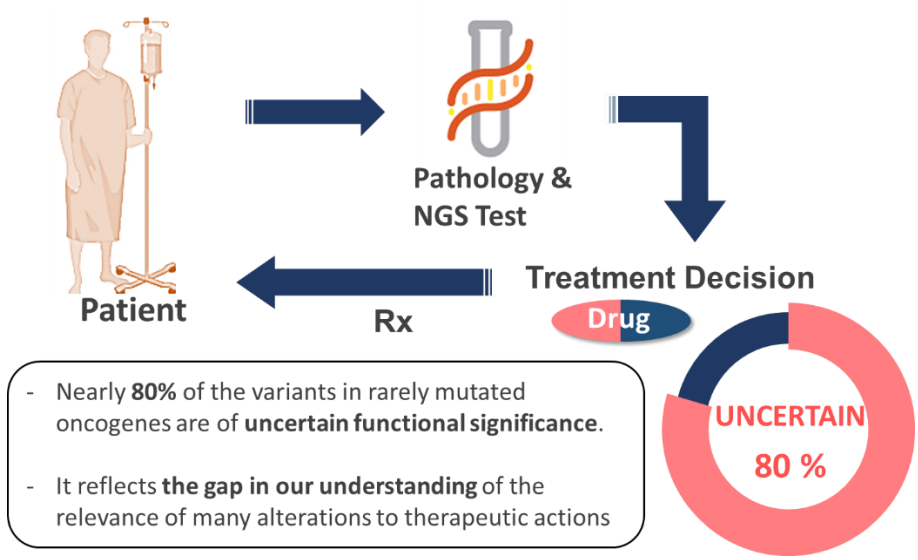


Figure 1.2 Current workflow of diagnostic (Dx) and Treatment (Tx) decision by doctors in the hospital using patient's pathology and NGS test result. Advances in sequencing technology have not been able to achieve personalized cancer patient's

care yet according to the study.

According to recent study, it is expected to revolutionize cancer therapy by the help of comprehensive genomic profiling[6,7]. A recent study showed that more than 90% of The Cancer Genome Atlas samples have potentially targetable alterations, the majority with multiple events, indicating that the challenges for treatment priority given the complexity of the genomic landscape.[8,9] Nearly 80% of the variants in rarely mutated oncogenes are of uncertain functional significance, reflecting the gap in our understanding of the relevance of many alterations potentially linked to therapeutic actions.[10] Although molecular alteration, revealed by most recent NGS sequencer, have been driving discovery of anticancer drug and development for more than several decades, with substantial progress in recent years, the comprehensive genomic test for medical oncologists to plan to optimally prescribe personalized therapy by matching every possible gene alteration to targeted agents remains largely unknown.

Identification of somatic genetic driver alterations in tumors can direct selection of effective targeted therapies. While advances in sequencing technology and target identification have had a major impact, only a small portion of cancer patients are treated based on the specific genetic mutations identified by sequencing. In addition,

responses to targeted therapies among genetically defined patients are heterogeneous. Prescribing therapeutics according to genetic mutations is limited by the current level of an incomplete understanding of the relationship between tumor genotype and drug sensitivity. Moreover, the opportunity represented by rare, exceptional responders in unselected patients is not exploited by current patient selection strategies (Figure 1.2).

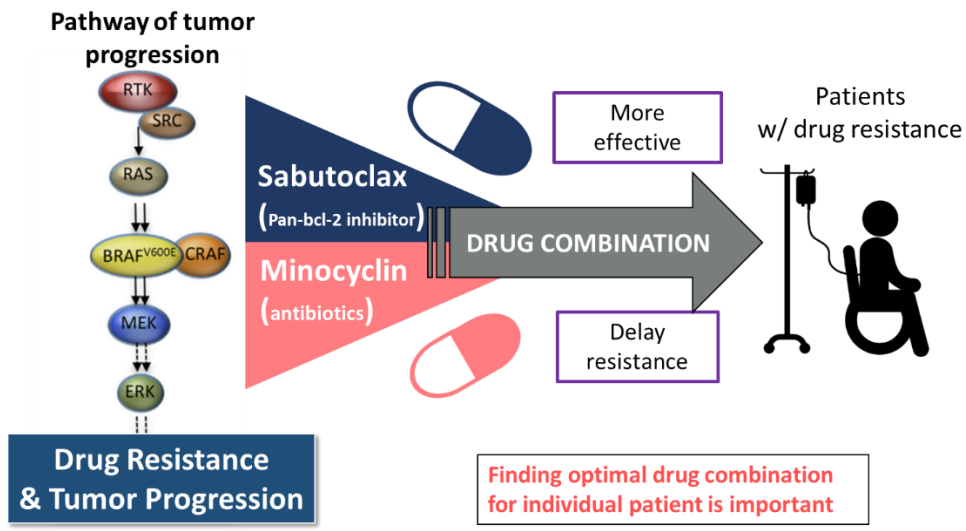


Figure 1.3 For terminal cancer patients having multiple drug resistance, combinatorial therapy is the last resort.

However, for many terminal cancer patients having multiple acquired drug resistance due to long-term treatment of a certain or multiple anticancer drugs, they have to find optimal drug combination that is effective in suppressing tumor progression and delaying drug resistance. Unfortunately, the patient's status is continuously changed during only short period of time especially for terminal-cancer patients. Treating optimized therapy to these patients can be the last option to save lives.

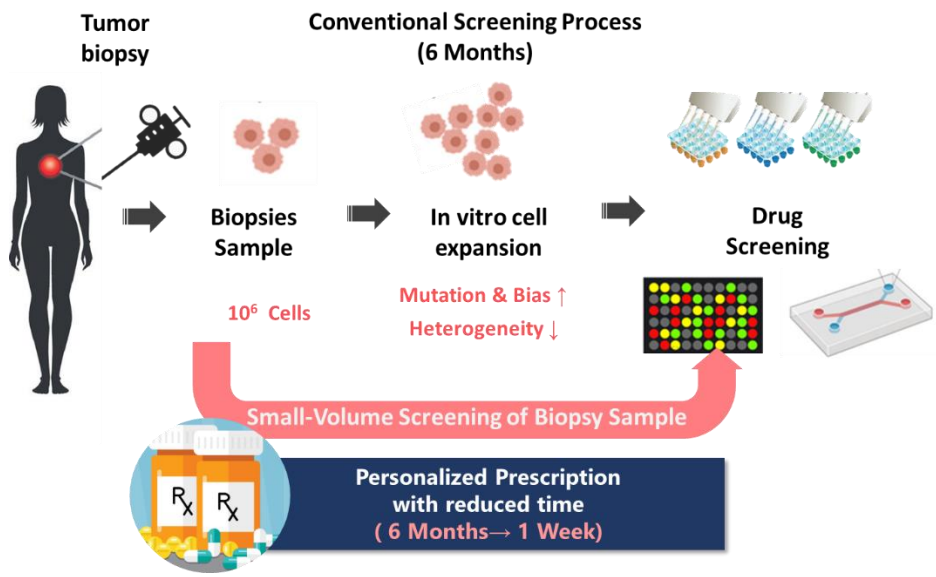


Figure 1.4 For personalized patient care to terminal patients, HTS using small number of cells has clinical value by reducing time to prescription of optimal drug

to them.

Combinatorial drug screening with cancer cells from the patient's biopsy and prescribing personalized medicine based on the screening result is one of the few solutions for cancer with highly progressed acquired resistance [4]. Such screening generally requires unbiased large-scale screening of numerous drug combinations, but the number of cells in the biopsy samples from patients that are typically comprised of $10^6$ cells or less is insufficient to obtain clinically meaningful results using conventional microtiter plate based platforms (Figure 1.2) [5]. Because of the lack of available cells, the process for establishing patient-derived cell (PDC) line is required to expand and secure enough number of cells for clinically meaningful screening results. This process normally takes 1-3 months for PDC establishment and 3-6 months to PDC expansion. Unfortunately, the patient's status is continuously changed during that period, and the survival rate is decreasing [5]–[8]. Moreover, the process of establishing a cell line is biased toward a specific subpopulation and lose heterogeneity of the original tumor. During the PDC expansion, bias and mutation have been accumulated, and the cell line becomes increasingly difficult to reflect the original state of the patient. Therefore, techniques for performing drug screening in the early stage with a small number of primary cells is essential to obtain

clinical benefits.

As shown in above Figure, when conventional HTS platform using 96-well plates, less than 10 drugs can be screened with primary cells from a biopsy. Therefore, in order to apply this concept of personalized therapy, it is needed to develop an appropriate small-volume HTS platform.

## 1.2 Competing technologies and Previous works

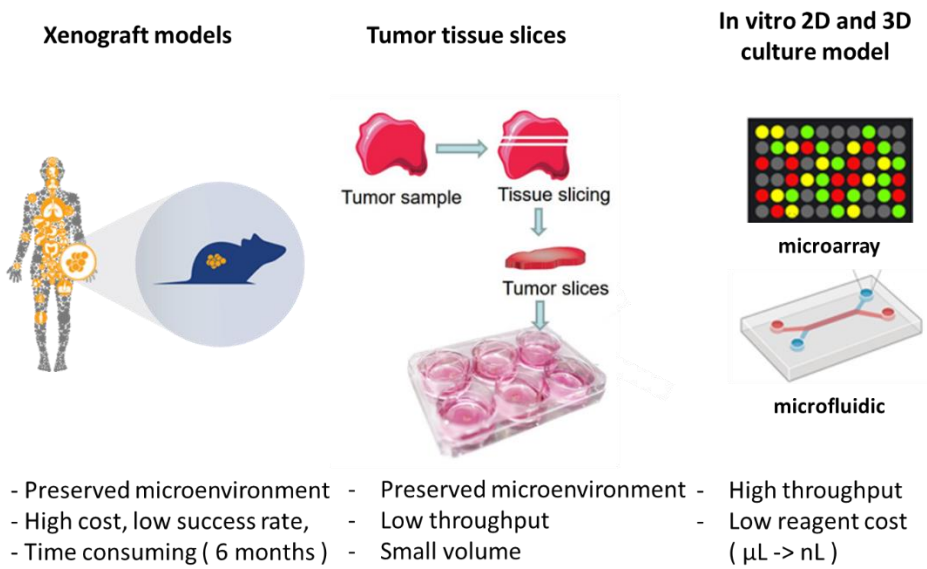


Figure 1.5 Current competing technologies for in vitro drug screening using patient-derived cells to find optimal drug treatment plan.

Finding effective drug combinations for a patient generally requires unbiased large-scale screening . However, the amount of cells obtained from a patient is usually limited; thus, only a few combinations can be tested for those samples using conventional high-throughput screening (HTS) platforms (i.e. 96- or 384-well-plate-based platforms) [16,17]. To overcome this limitation, various types of HTS platforms have evolved to reduce reaction volume, thereby decreasing the consumption of valuable cells and reagents [18–21]. These platforms only need

nanoliter or picoliter amounts of reagent and a few hundred cells per reaction, thus making possible large-scale drug screening with patient-derived samples [16,17]. However, as the screening platform becomes miniaturized and the scale of screening expands, increasingly sophisticated and expensive liquid handling systems are required for managing a large number of drug candidates to be tested [22]. Because the majority of hospitals and laboratories worldwide have difficulty securing proper infrastructure and extra funding to operate such a high-cost liquid handling system, it is challenging for them to utilize HTS for clinical applications and academic studies [16,17].

Ex vivo tests on primary patient-derived tumor samples include xenograft models, tumor tissue slices, and 2D and 3D culture models. First, fresh pieces of tumor are implanted into immunodeficient mice aiming to follow the dynamics of tumor progression during and after treatment. Xenograft models are important for pre- and co-clinical evaluation of anticancer treatment. However, there are also disadvantages in using xenograft models. First, the success rate of establishing of a xenograft is low. Second, this method is very costly and not compatible with high throughput required in precision medicine. And third, the time of establishing varies from 2 to 12 months, normally it takes at least 6 months to establish PDX model. These drawbacks restrict their clinical applications for making decisions about the appropriate therapy.

Second, tumor tissue slices are thin slices of a tumor that are tested in microwell plate with different compounds. The advantages of this model are that tumor cells are preserved in their original environment and their response to drugs can closely represent tumor response in vivo. The model is, however, only limited to patients that undergo a surgery. Moreover, this is a low throughput method limiting the number of possible compounds and combinations that can be tested.

In vitro 2D and 3D cell culture models are most promising to be adopted for testing of patient-derived cells in clinics, due to their compatibility with high throughput, possibility to be performed within 1 week, and requirement of relatively small volume of cells. Performing such in vitro sensitivity tests as a routine in clinical practice will open a new era of precision medicine in oncology and will help to navigate the decision making toward successful therapy for each individual patient. Thus, in this dissertation, I mainly focus on study of in vitro miniaturized drug testing platform on cancer cell line or patient-derived cells.

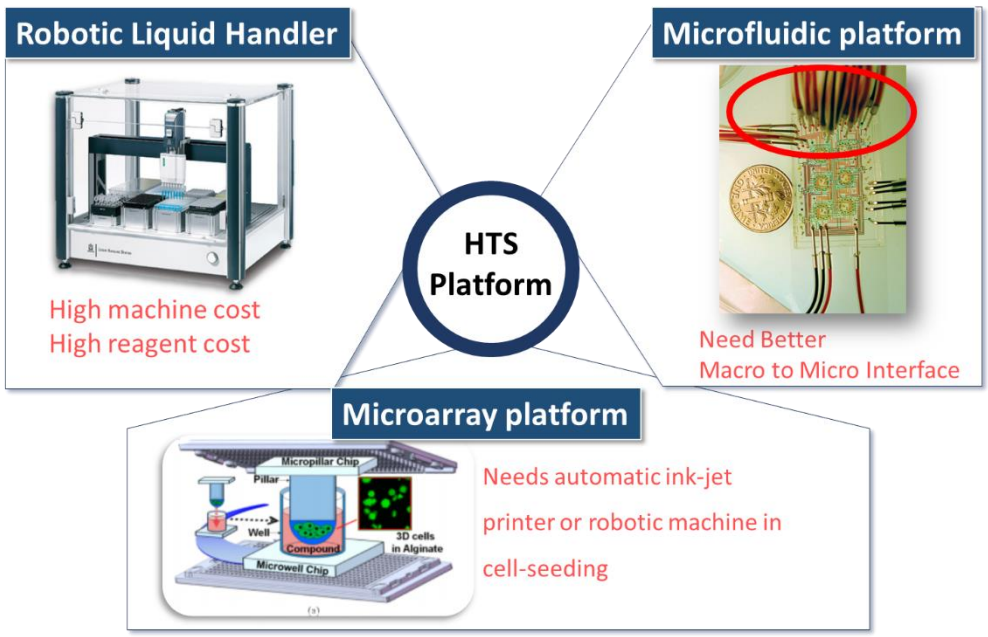


Figure 1.6 Previous in vitro culture models have limited use for translational platform in terms of user-friendliness and cost.[11]

In high-throughput assay, push to increase throughput and miniaturize assays has resulted in the need to be able to dispense sub-microliter volumes of liquids accurately and precisely. But dispensing such small volumes can be a challenging and require lots of workload especially when high-throughput screening assay is needed in their experiment.

The first option to overcome these limitations is to use robotic liquid handler. Pharmaceutical industry and more recently academic research and clinical diagnostics have adopted to utilize automated liquid handling systems to add improved consistency and increased efficiency in the high throughput screening process. However, the cost of setting up such a system can be expensive and for high-throughput screening to be operated using conventional 96-, 384- well plates, the relevant reagent cost is also expensive. Thus, many small- and medium-sized laboratory still could not afford the robotic liquid handler.

As an alternative approach, many Lab-on-a-chip-based HTS platforms have been developed by the advantages of miniaturization, which helps to reduce the reagent volume. This enables to screen rare samples such as stem cells or patient derived cells. However, Lab-on-a-chip-based HTS platforms are still much to be desired for individual laboratory to fully utilize, since many Lab-on-a-chip-based platforms require expensive automatic liquid handlers and complex operation methods. Of the two major types of Lab-on-a-chip-based platforms, microfluidics-based platforms should accompany complex instrumentation such as convoluted valves, tubing, and microfluidic controllers.[12,13]

Microarray-based platforms, an alternative approach using lab-on-a-chip technology,

also need high-cost equipment such as microarray spotter or pico-liter injector to print drug molecules on the substrate of microwell array. For these reasons, current lab-on-a-chip-based HTS platforms are difficult to be used in small-scale laboratories desiring to perform large-scale drug screening with restricted resources.[11,14–17]

## 1.3 Main Concept: *In vitro* drug testing using miniaturized encoded drug-laden hydrogel array technology

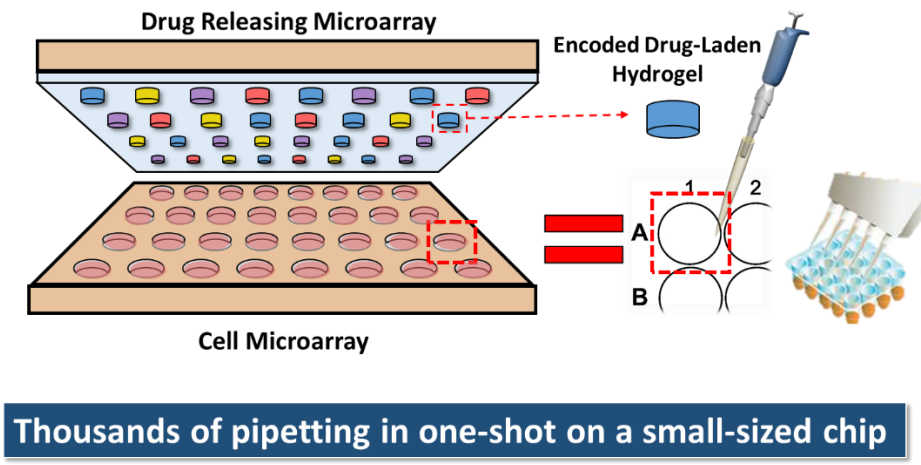


Figure 1.7 A schematic illustration of in vitro drug testing platform using drug-laden hydrogel microarray.

A novel multiplexed bioassay method, named as 'Partipetting', represents one-step pipetting of heterogeneous encoded drug-laden microparticles (DLPs) and self-assembly of DLPs into microwells. Face-to-face assembly of DLPs-attached chip with target Cell chip enables large-scale parallel bioassays. The proposed platform has several advantages to making it easier for users to perform the process from drug preparation step to large-scale screening operation.

First, encoded DLPs library can be prepared by just transferring drug solution from commercial drug library, which can be purchased in a multi well-plate format, to the well-plate filled with prefabricated microparticles, followed by freeze-drying. Second, the total workload increases linearly, not exponentially, as sequential screening progresses. For the m-step library to library screening, only m-step pipetting is needed regardless of the total number of drugs in each step. This can drastically reduce time-consuming and lighten the burden of drug screening. Third, it is hand operable large-scale screening platform. This offers more approachable platform to individual researchers compared with previously proposed platform based on lab-on-a-chip technology, since automatic liquid handler is essential to satisfy the enormous number of liquid handling operation when previous HTS platforms is used.

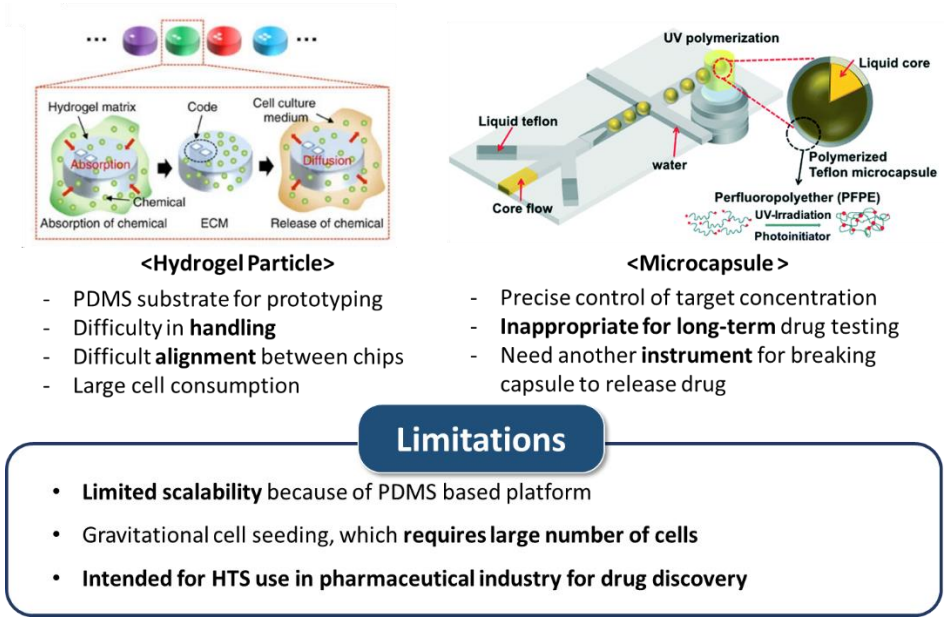


Figure 1.8. Previous work on miniaturized HTS platform in our group.

Our group has been investigating two different type of miniaturized in vitro drug screening platform. Both type depends on miniaturized microarray-based platform. And the difference can be explained in terms of what type of drug-laden particles(DLPs) are adopted in each of the platform.[18–23]

The first type utilized hydrogel particle as its DLP, the hydrogel particle impregnated with chemical compounds using simple absorption-based drug loading. The advantage of this DLP is that the loading process was quite simple. Drug molecules dissolved in aqueous solution are absorbed into the hydrogel particle and make it dry

for chemical compounds to be absorbed in the hydrogel.[24]

The second type utilizes liquid-capped microcapsule like core-shell structure. Teflon-shell and core-of drug solution is generated by using droplet microfluidics. This system is advantageous for delivering the desired amount of drug precisely, and the high loading amount is available. However, the fabrication process of encoded liquid microcapsule is sophisticated so that it is hard to scale-up the fabrication process. Also, the Teflon-shell is so tough that it is hard to rupture the shell structure. It needs another equipment to mechanically break the shell meaning that it requires another costly instrument. The most important drawback is when microcapsule is combined into one microwell seeded with target cell line during incubation for drug testing, the microcapsule occupies relatively large volume of microwell so that the space of media become relatively short of. And this leads to the failure of long-term drug testing due to the shortage of cell culture media.[22]

In this dissertation, to overcome these drawbacks from previous proposed miniaturized in vitro drug testing platform, I propose large-scale drug-laden hydrogel array-based in vitro drug testing platform. The detailed contents in this dissertation are as follows

In chapter 2, I will explain in detail the development of whole system for miniaturized in vitro drug screening platform using array technology of heterogeneous encoded drug-laden hydrogel. In chapter 3, I will demonstrate sequential anti-cancer drug combination test on cancer cell line as an application study. In chapter 4, I will present simultaneous anti-cancer drug combination on lung cancer patient-derived cell line acquired from biopsied sample of patients to demonstrate developed platform working in small-volume assay. In chapter 5, I will demonstrate the engineering of Cell Chip part to become 3d-culturable platform which opens possibility to test 3d spheroid or organoid.

# Chapter 2 Platform Development of Drug Releasing Hydrogel Microarray

In this chapter, I present the development of drug releasing hydrogel microarray. First, I introduce how to fabricate drug-laden hydrogel microparticles. Drug loading method and how to obtain uniformity and linearity of the profile of the drug-loaded microparticles. Then, I explain how to construct heterogeneous drug-laden hydrogel microarray. Lastly, I validate the biocompatibility of cells cultured in this platform and isolation of microwell.

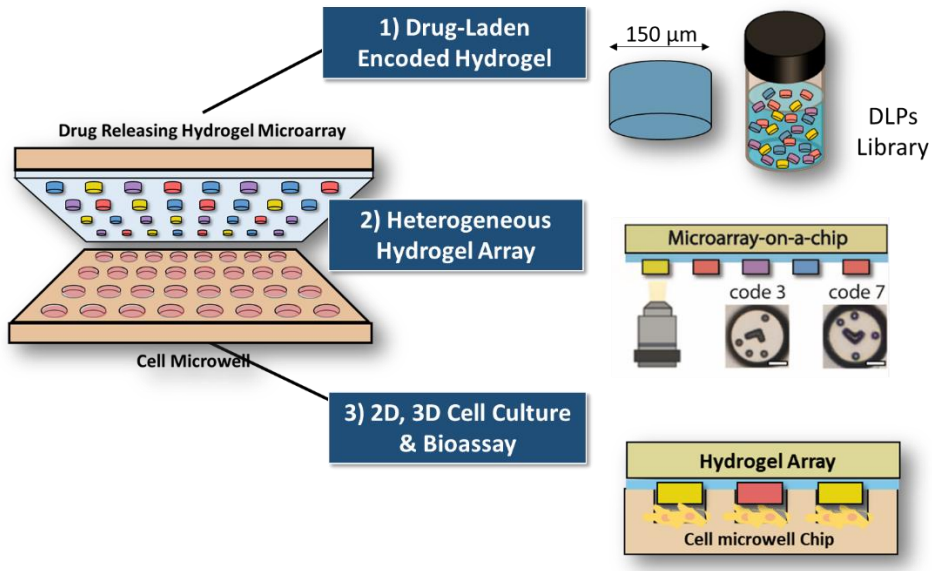


Figure 2.1. Platform Overview. Platform can be largely divided into three subgroup; 1) Drug-laden encoded hydrogel, 2) Heterogeneous hydrogel array, and 3) 2D, 3D cell culture & bioassay.[23]

## 2.1 Encoded Drug-Laden Hydrogel & Library Construction

### Fabrication of encoded microparticle via photopolymerization

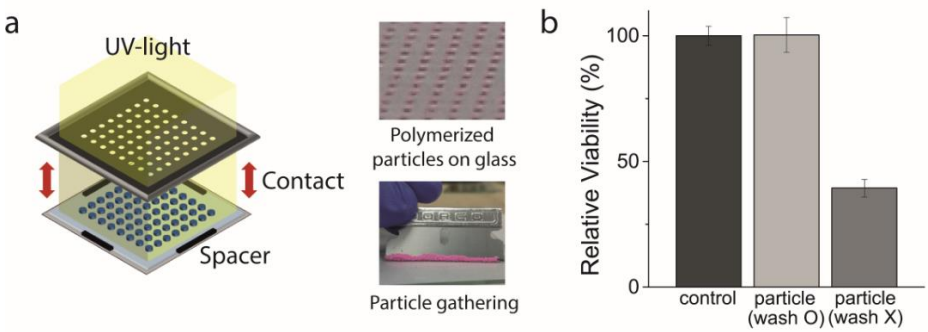


Figure 2.2 Fabrication process of encoded-drug-laden particles (DLP) and its effect on the viability of target cell line. (a) Encoded hydrogel microparticles were fabricated by mask photolithography. 45μm of spacer was applied to adjust the height of microparticles. 15,225 microparticles were polymerized simultaneously on a single mask, and polymerized microparticles were collected into a 1.5 ml-volume centrifugal tube by scraping them with razor blade. ( Reprinted from [21] )

Encoded hydrogel microparticles, which are used as drug carriers, were fabricated by photolithography with a photocurable polymer (polyethylene glycol diacrylate, Mn 700). These particles have a diameter of 138 μm and a thickness of 38 μm. Polymerized hydrogels were washed with ethanol two times to remove uncured monomer and easily collected into the test tube or well plate using a blade (Figure 2.2a). No cytotoxicity caused by hydrogel microparticles was found (Figure 2.2b). A

library of drug-laden hydrogel microparticles could be prepared in a simple and highly parallel manner, which is described as follows. The drug solution was added into the microwells with prefabricated microparticles, and the solvent was removed by freeze-drying. Because commercial drug libraries are generally supplied in a 96- or 384-well plate format and microparticles can also be supplied in a well plate format, the DLPs-supplier or the end-user only needs to transfer the drug solution and freeze-dry the mixture. After complete drying, the microparticles in each microwell were collected together into inert silicone oil to construct a DLP library. Here, silicone oil prevents cross-contamination between different DLPs and functions as delivering liquid during the partipetting process.

As opposed to our previous study on the partipetting platform, I adopted the freeze-drying-based drug loading method in this study to attain a uniform and high amount of drug loading regardless of the drug or solvent type. With Rhodamine-B as a model substance, I investigated the loading uniformity by measuring the fluorescence intensity of microparticles (Figure 2.3). The loading uniformity from the previous method (gray), was 30.6%. It was improved by 6.19% by freeze-drying (red). The amount of drug molecules that could be delivered to a microwell with a single microparticle could be estimated from a bulk-scale loading-releasing experiment (Figure 2.3). After drug loading, 1.5 mL of Phosphate-buffered saline

(PBS) solution was added to DLPs and then the mixture was shaken on a mixing block overnight, which was enough time for complete release (Figure 2.3). I set the volume of PBS solution to make the particle-number (15,225) to releasing volume (1.5 mL) ratio equivalent to the ratio of a single particle to the volume of one microwell on the cell chip (100 nL). The concentration of the released solution was measured from an ultraviolet-visible absorbance spectrum. As a result, I validated that the released amount of drug molecules was linearly proportional to the initial loading amount (Figure 2.3). Therefore, once the releasing ratios of the drugs were examined, I could easily modulate the target concentration by controlling the loading amount of the drugs.

The detailed fabrication protocols is as follows : Encoded microparticle fabrication: Encoded hydrogel microparticles were fabricated via UV photolithography (OmniCure S1500, Excelitas Technology Corp.) with poly(ethylene glycol)-diacrylate (PEG-DA, Mn=700; Sigma-Aldrich) and 5 wt% photoinitiator (2-hydroxy-2-methylpropiophenone 97%, Sigma-Aldrich). To generate different codes for each hydrogel microparticle, different masks (MicroTech, South Korea) with the capacity to generate 15,225 microparticles at once were used. Here, each microparticle had a diameter and thickness of 138 μm and 38 μm, respectively. All the fabricated hydrogel particles were first collected in ethyl alcohol (EtOH) solution.

To prevent the remained photoinitiator of uncured resin from damaging cells, the washing steps with ethanol solution were repeated two times.

**Drug Loading Method**

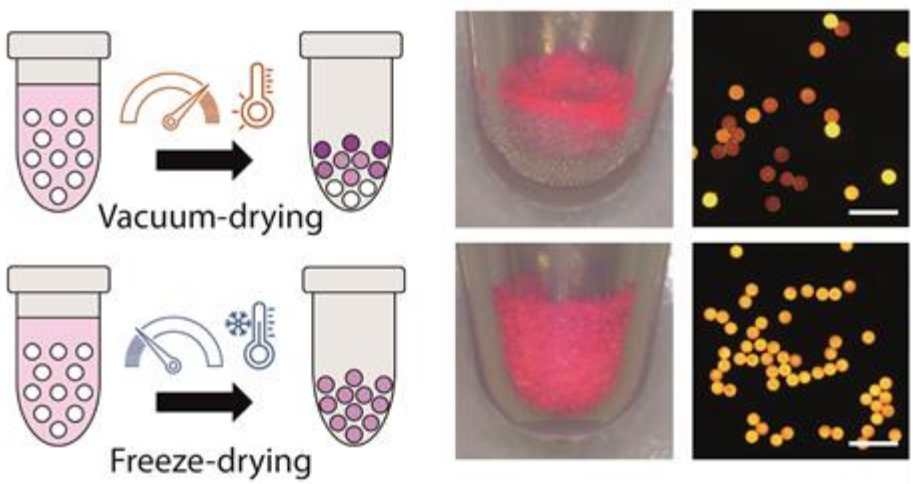


Figure 2.3 Drug loading into the prefabricated encoded hydrogel microparticles using freeze-drying method. A schematic of drug loading method is presented in comparison with conventional vacuum-drying method (Left) and the bright-field and fluorescent image of each group of microparticles loaded with Rhodamine-B by two different drug loading method are presented. ( Reprinted from [21] )

Contrary to the drug-loading method of solvent evaporation using simple drying in a vacuum in the previous study on the partipetting platform, I changed from solvent evaporation method to the freeze-drying-based drug loading method in this study to guarantee the uniformity of drugs loaded on microparticles independent of drug or solvent type. To visually demonstrate the degree of variation in drug concentration of each drug-loaded particle, I used Rhodamine-B as our model fluorescence chemical. The loading uniformity of drug-laden microparticles in a tube was investigated by measuring the fluorescence intensity of microparticles.

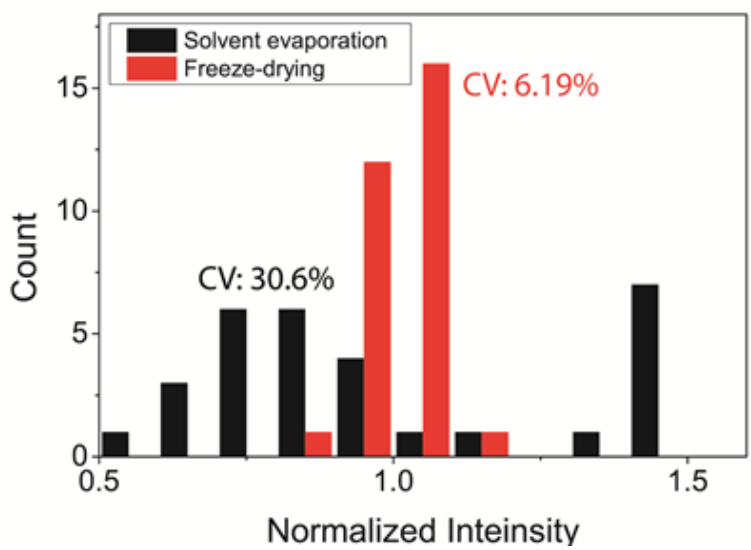


Figure 2.4 Comparison of the uniformity by two different drug-loading method. ( Reprinted from [21] )

Based on measuring fluorescence of rhodamine B-loaded microparticles, the loading uniformity between the methods of solvent evaporation and was shown in the above chart. The loading uniformity can be interpreted as inversely proportional to the value of coefficient of variation (CV). The CV value of the previous method (solvent evaporation, gray) was 30.6% and that of the newly suggested method( freeze-drying method, black) was 6.19%. By comparing the value of coefficient of variation between two different method, I could identify that the freeze-drying method is superior than conventional solvent evaporation method from the perspective of loading uniformity (Figure 2.4)

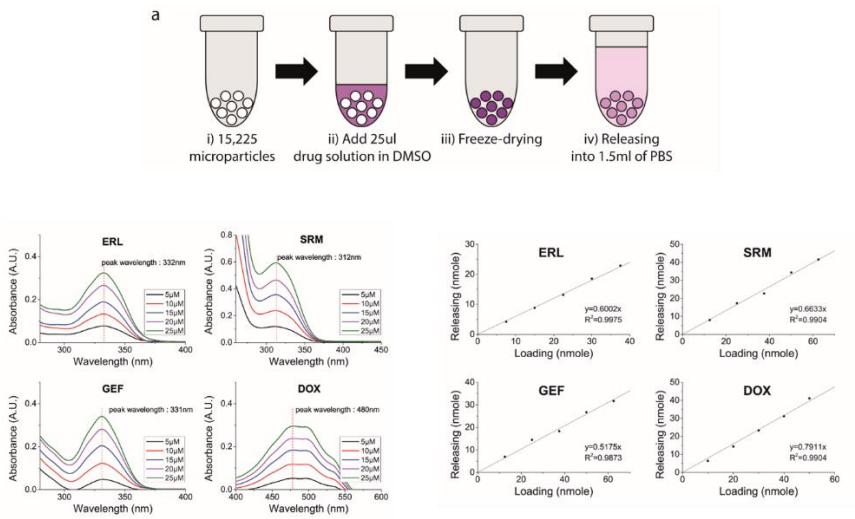


Figure 2.5 The optimization process of released concentration from drug-laden hydrogels and its uniformity in concentration. Drug Loading-releasing relationships are presented for some representative drugs used in this experiment. ( Reprinted from [21] )

The amount of drug molecules that could be delivered to a microwell with a single microparticle could be estimated from a bulk-scale loading-releasing experiment. After drug loading, 1.5 mL of Phosphate-buffered saline (PBS) solution was added to DLPs and then the mixture was shaken on a mixing block overnight, which was enough time duration for complete release. I set the volume of PBS solution to make the particle-umber (15,225) to releasing volume (1.5 mL) ratio equivalent to the ratio of a single particle to the volume of one microwell on the cell

chip ( approximately 100 nL ). The concentration of the released solution was measured from an ultraviolet-visible absorbance spectrum. As a result, I validated that the released amount of drug molecules was linearly proportional to the initial loading amount. Therefore, once the releasing ratios of the drugs were examined, I could easily modulate the target concentration by controlling the loading amount of the drugs. (Table). Preparation of drug-laden microparticles (DLPs) and measuring drug releasing ratio: Erlotinib hydrochloride and Gefitinib (free base) were purchased from LC laboratories, and all other chemical drugs were purchased from Sigma Aldrich. Drug concentration was measured with an ultraviolet-visible spectrophotometer (UV-1800, Shimadzu). First, the peak wavelength of absorbance spectrum was measured for each drug (Figure 2.5). Subsequently, a reference curve for the relationship between the drug concentration and corresponding absorbance peak was obtained using samples with a known concentration. Then, the concentrations of the unknown samples can be calculated from the reference curve (Figure 2.5). To evaluate the drug releasing ratio of each drug, the following procedure was conducted. First, 25 μl of drug solution (dissolved in DMSO) at a known concentration was added to 15,225 microparticles, which were fabricated from a single mask. After freeze-drying, 1.5 mL of PBS solution was added to drug-laden microparticles, and then the mixture was shaken on a mixing block (MB-102, BIOER) overnight, which was enough time for complete release. Next, the

concentration of released solution was measured. The particle-number (15,225) to releasing volume (1.5 mL) ratio was equivalent to the ratio of a single particle to the volume of one microwell (100 nl) (Table S2). I tried to eliminate the differences in releasing ratios that might occur depending on the particle numbers and volume ratios. Five data points for each drug were collected.

**Coding Scheme & its Decoding algorithm.**

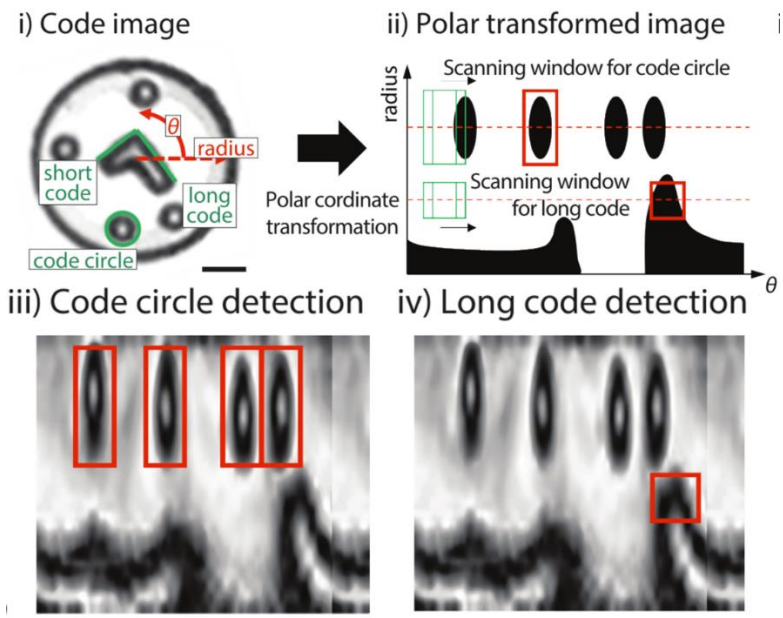


Figure 2.6. The automatic decoding process of code distribution are presented. Code design and decoding algorithm. i) ‚Long code' and ‚short code' are components for identifying the rotation and inversion of microparticles, respectively. The locations of four 'code circles' determine the code number. Ii) Particle image is transformed into polar coordinates, and the locations of each code component are recognized by a machine learning based algorithm. iii) and iv) are example images of recognizing code circles and long code, respectively. ( Reprinted from [21] )

To identify which drug was treated on each microwell from randoml y assembled DLPs, I utilized coding scheme on fabricated microparticles and developed automatic code reading software (Figure 2.6**).** The scheme of enc oding on microparticle for bioassay was considered in terms of coding capac ity and distinguishability. The proposed schemeshould offer enough high codi ng capacity that is capable to cover the number of possible drug library and it should be easily distinguishable when the encoded particle is inverted, ro tated, and partially damaged. Then,coding scheme are presented in the Figur e 2.6. and Each coding component can be described as follows : Three cod e elements were used to construct the graphical barcode (Figure 2.6). The ‘l ong code’ and ‘short code’ were utilized for analyzing the rotation angle an d upside-down inversion of particles, respectively. ‘Code circles’ were used f or determining code numbers. For the reading process, first, the detected par ticle image was transformed into polar coordinates, and the positions of the code circles and the long code were recognized in the scanning window trav ersing the scanning line (Figure 2.6). Short codes can be easily detected by comparing the intensity of the area at -90 degrees and +90 degrees from the long code position (θ). With these code element locations, the code of the particle was finally determined. By using neural-network-based image recogni tion and subsequent error-correction procedure, more than 95% of the particl

es were successfully decoded. The error under the 5% includes the broken p articles whose code cannot be decoded. Finally, a sequential combinatorial c ode map was constructed by combining the code maps of the first and seco nd chips.

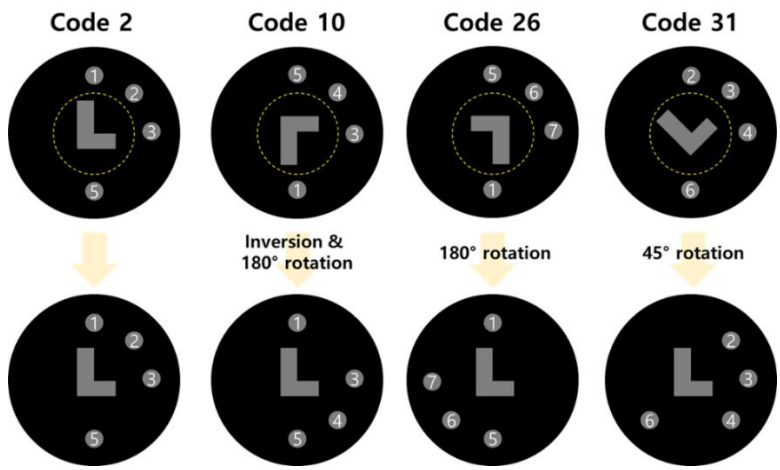


Figure 2.7 Detailed encoding scheme under different situation. Long code and short code are designed for alignment in code reading of encoded microparticles.

In the Figure 2.7, detailed coding & decoding scheme are explained under a variety of situation such as flipped, rotated. If we first recognize ‘long nose’ and ‘short nose’ for reference, then we could identify the code of the hydrogel particle by analyzing the pattern of the distribution of four dots.

## 2.2 Array generation of heterogenous drug-laden microparticles.

**Particle Chip & Transfer Chip**

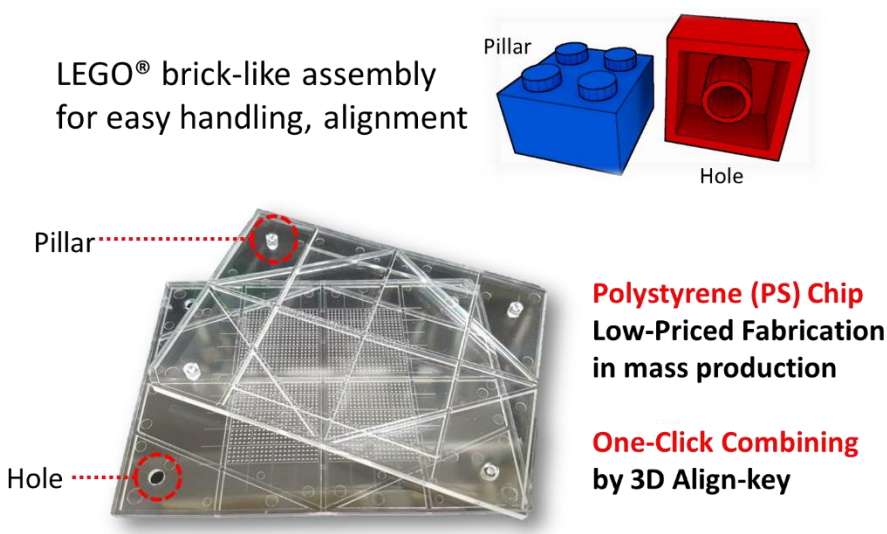


Figure 2.8 Plastic chip for mass production and Low-priced fabrication was made by Injection Molding

Drug molecules in hydrogel microparticles start to diffuse out after a microparticle touches a cell culture medium. During the incubation, each microwell should be completely isolated to prevent cross-contamination. This diffusion was

validated with Rhodamine-B. The impregnated molecules in the microparticle were gradually released into the surrounding solution, and the releasing process was completed within approximately 30–60 min. I also ensured that the isolation of each microwell was maintained perfectly for at least 1 day. If the releasing speed was too fast, cross-contamination between microwells would occur during the chip assembly process, which requires around 5 s. On the contrary, if the releasing speed were too slow to finish the releasing process within the drug incubation time, it would be difficult to obtain accurate assay results. Considering that the incubation time for an anticancer drug assay is usually more than 10 h, the releasing speed of our hydrogel microparticles is acceptable for use in drug screening. Conversely, the sealing of microwells may inhibit gas exchange during the incubation period, which could affect the cell status. To understand this potential impact, I investigated the influence of sealing the cells in terms of cell morphology and viability, and there was neither a morphological change nor a decrease in the survival rate due to sealing.

## 2.3 Cell Culturing on Cell Chip and bioassay

### 2D Monolayer Cell Culture

For the cell-based assay, cells were seeded on the 'cell chip', which has microwells with a diameter of 600 μm and a depth of 350 μm. The gravitational settling method or sealing film assisted seeding method was used for cell plating (Figure 2.9). Sealing film assisted the seeding method, which could reduce cell consumption, was developed for potential applications in rare cell screening, such as seeding stem cells or patient-derived cells (Figure 2.9). Cell seeding on 1,600 microwells was available only with 320 μl of cell suspension, which was two times more than the total volume of 1,600 microwells. Effectively, approximately 200 cells were required for seeding 100 cells per microwell. This seeding method could be completed within 10 seconds, and the seeding uniformity was within 10% of the coefficient variation. After preparing the cell chip and drug-releasing hydrogel microarray-on-a-chip, both chips were combined in a face-to-face manner to conduct multiplexed cell-based bioassays. Sequential treatment assays were available by simply replacing the microarray-on-a-chip after incubation.

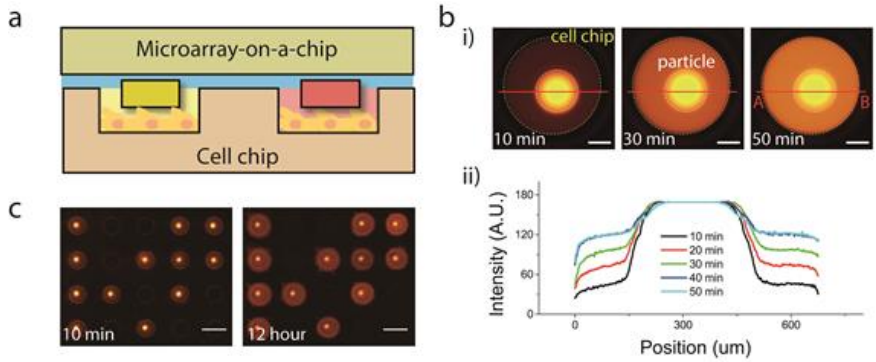


Figure 2.9 Drug releasing into microwells and isolation of each microwell during incubation. (a) Schematic of combining Cell chip and drug-releasing hydrogel microarray. PDMS layer prevents the leakage between microwells. (b) Time-lapse drug releasing profile. Rhodamine-B was used as a model chemical. The releasing process was completed within approximately 30 minutes to 1 hour. i) Image of microwells with Rhodamine-B releasing microparticle. The fluorescence intensity profile from 'A' to 'B' is presented in ii). Scale bar: 150um. (c) The isolation of each microwell was maintained well more than 12 hour incubation time. Scale bar: 1mm. ( Reprinted from [21] )

Drug molecules in hydrogel microparticles start to diffuse out after a microparticle

touches a cell culture medium. During the incubation, each microwell should be completely isolated to prevent cross-contamination. This diffusion was validated with Rhodamine-B (Figure 2.9). The impregnated molecules in the microparticle were gradually released into the surrounding solution, and the releasing process was completed within approximately 30–60 min. I also ensured that the isolation of each microwell was maintained perfectly for at least 1 day. If the releasing speed was too fast, cross-contamination between microwells would occur during the chip assembly process, which requires around 5 s. On the contrary, if the releasing speed were too slow to finish the releasing process within the drug incubation time, it would be difficult to obtain accurate assay results. Considering that the incubation time for an anticancer drug assay is usually more than 10 h, the releasing speed of our DLPs is acceptable for use in drug screening. Conversely, the sealing of microwells may inhibit gas exchange during the incubation period, which could affect the cell status. To understand this potential impact, I investigated the influence of sealing the cells in terms of cell morphology and viability, and there was neither a morphological change nor a decrease in the survival rate due to sealing.

**Well-to-well isolation during incubation**

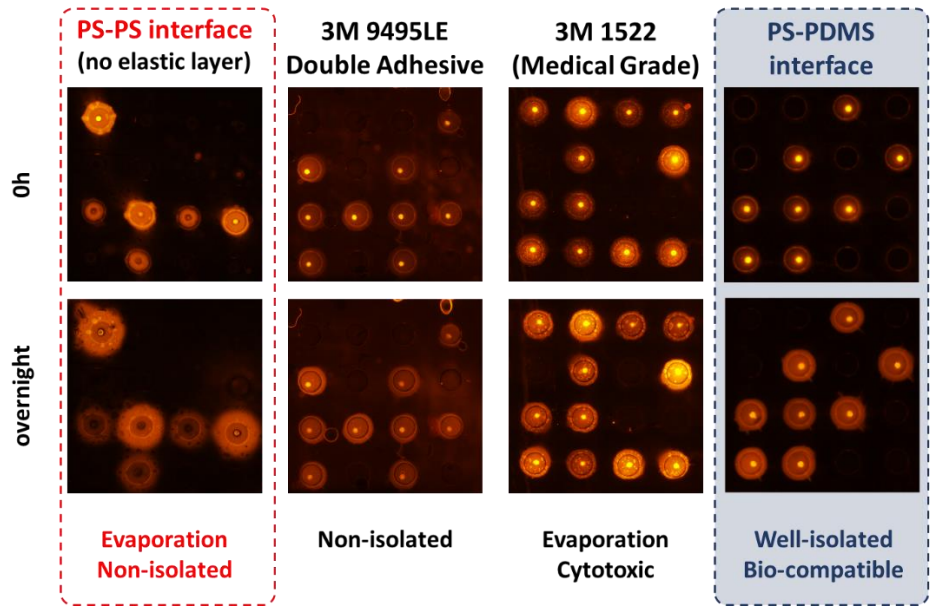


Figure 2.10. PDMS layer showed the best performance in well-to-well isolation

And I also confirmed that this microarray-based platform has a good isolation performance under PDMS layer was used. And is it compared with other groups of commercially available adhesive layer ( Figure 2.9.)

# Chapter 3 Sequential Drug Combination Screening Assy on TNBC

**Platform Validation with Applicational Study**

In this chapter, I present an application of in vitro drug screening platform developed in this dissertation. I demonstrated sequential combinatorial drug screening of a targeted inhibitor followed by genotoxin against 'triple-negative' breast cancer (TNBC), which is especially known as a highly resistant from a breast cancer. First, I will briefly introduce the background and the motivation regarding the strategy of treating sequential drug combination. Second, I will present experimental design and relevant technical issue in the application of this platform to sequential drug combination assay. Then, I will explain technical issue and our engineering solution for handling the issue. technical issue in  Finally, I found the most promising sequential drug combination pair out of 45 possible combination from the library.

## 3.1 Background : Sequential Drug Combination as promising therapeutic option

Treatment of diseases with multiple drugs allows for more complex and sophisticated cellular pathway regulation.[25,26] Thus, finding effective drug combinations has long been of interest, and these combinations have been applied to cure patients with resistant cancers, who were difficult to treat with single drug therapy. However, simultaneous administration of multiple drugs increases dose exposure to patients at a specific moment and therefore has significant potential to result in side effects.[25,27] To address this limitation, sequential treatment with multiple drugs has received much attention. Recently, several studies have reported sequence-dependence of some drug combinations, which are more potent than simultaneous combinations. The basic principle is the dynamic redistribution of intracellular pathways that make pretreated drugs vulnerable to post-treatment drugs. When these effective sequential combinations are found for each patient, resulting in personalized medicine, they not only provide a promising therapeutic effect, but also help improve the quality of life by reducing the dose of the drug given to the patient.[28,29]

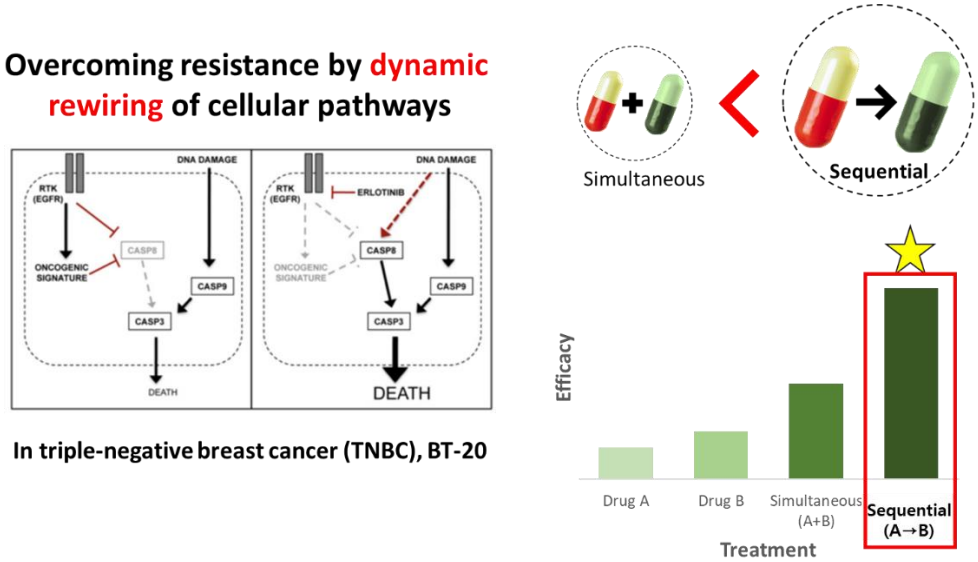


Figure 3.1 Sequential drug combination is a promising strategy acting synergistically for many patients.[28]

## 3.2 Experimental Design with sequential drug treatment assay

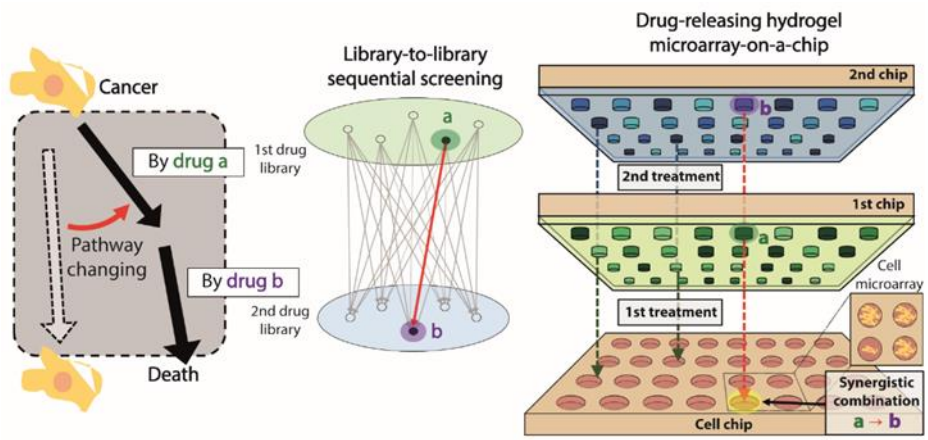


Figure 3.2 A schematic image of sequential treatment achieved with partipetting platform by replacing a chip like a printer cartridge format.. ( Reprinted from [21] )

To perform sequential drug treatment combination screening, we use the developed drug screening platform using drug-releasing hydrogel microarray for sequential screening on TNBC cell line, which is known as most incurable type of breast cancer cell, not having the drug targeted for FDA-approved targeted therapy.[30] Based on the platform developed and described in Chapter 2, sequential drug screening was achieved.

## 3.3 Technical Issue & its engineering solution

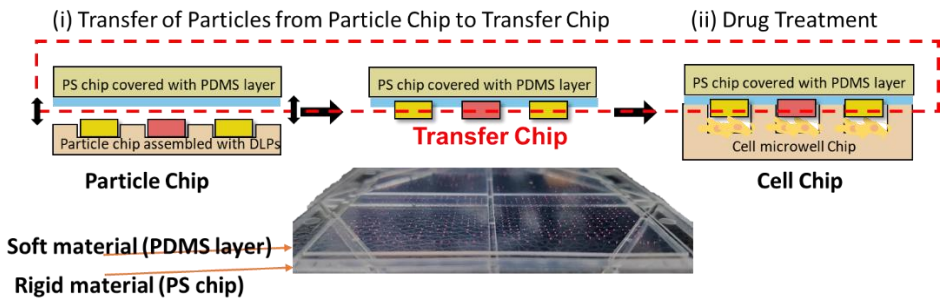


Figure 3.3 Transfer Chip was introduced for particle transfer and prevention of cross-contamination. An adhesive layer was applied on the Polystyrene chip, and assembled hydrogel microparticles array was transferred on the top of the layer.

Soft lithography using PDMS, a traditional manufacturing technique for microwells, is useful for prototyping, but too expensive and slow for mass production. In addition, the flexible and stretchable nature of PDMS makes it difficult to perform an accurate chip-to-chip alignment process between two combined microwell arrays. Therefore, the platform was made of polystyrene (PS) chips through injection molding. This is a strategy to easily expand rigid plastic components using a three-dimensional alignment key with pillar and hole structures,

making sequential replacement easy (Figure 3.3). However, PS chips can have micrometer-scale surface roughness, and this roughness on the PS chip surface can create a slight gap between the two combined microwell chips, causing cross contamination between adjacent microwells. Such cross-contamination can cause serious problems for microwell-based technology, as each microwell must be isolated and perform separate reactions. To solve this problem, I introduced a transport chip composed of a two-layer structure, and a PDMS layer, a biocompatible and flexible material to fill the gap, was placed on a solid PS chip (Figure 3.3). In particular, the attraction force between the PDMS and the fine particles made of PEGDA 700 is strong enough to persist even after one day of incubation. No additional surface treatment is required for the PDMS layer. We have manufactured a large set of PS chips capable of carrying out 1,600 parallel reactions within a 52mm x 52mm sized area by carefully controlling some parameters such as the depth and diameter of each microwell and the distance between adjacent microwells.

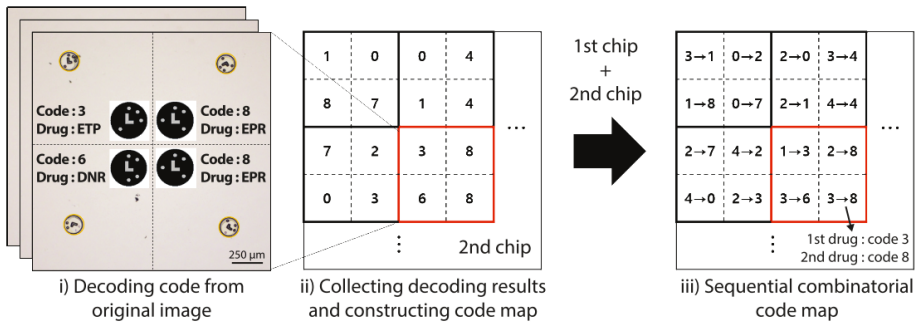


Figure 3.4 Code mapping process for sequential combination assembled randomly on particle chip. ( Reprinted from [21] )

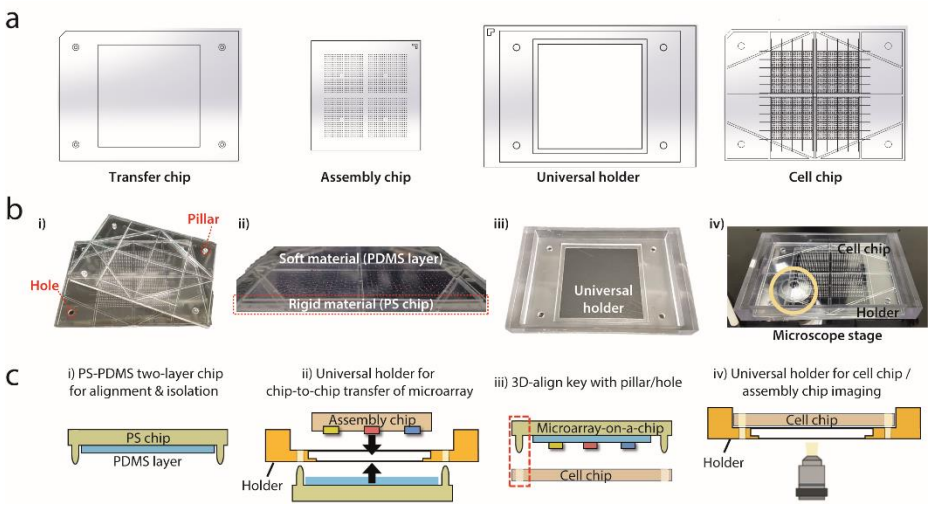


Figure 3.5 Large-Scale chip design and holder for user friendly interface. ( Reprinted from [21] )

A schematic illustration of how each polystyrene chip and the universal holder is used in each step is shown in experimental order (Figure 3.5). Assembled hydrogel microparticles on the assembly chip are transferred to the transfer chip with the help of a multi-purpose plastic holder (named a ‘universal holder’) for exact alignment. Then, large-scaled imaging for positional code mapping is performed. The imaging process is implemented on the universal holder, which is designed to be same size and compatible with the microscope stage for conventional 96-well plates; thus, all the microparticles are located at pre-set coordinates. Subsequently, combining the transfer chip (microarray-on-a-chip) and the cell chip induces drug release. In this process, pillars on the transfer chip and holes in the cell chip facilitate an exact alignment. After incubation, whole microwells on the cell chip with drug-treated cells are imaged on the top of the universal holder, thereby collecting viability information on the whole chip.

The detailed description of hip fabrication is as follows : All the plastic chips, including the assembly chip, transfer chip, and cell chip, were manufactured by plastic injection molding using an injection molder (Woojin Selex Co., Ltd, South Korea). An aluminum mould was made using a CNC milling machine (Hwacheon technology, South Korea). All the chips, which were made of polystyrene (GPPS, LGChem., South Korea), contained 1600 microwells. The microwells of the cell chip

had a diameter of 0.6-mm and a well-to-well distance of 1.5 mm. The microwells on the assembly chip had a diameter of 160 μm and a well-to-well distance of 1.5 mm (same distance as the wells on the cell chip).

## 3.4 Assay Result

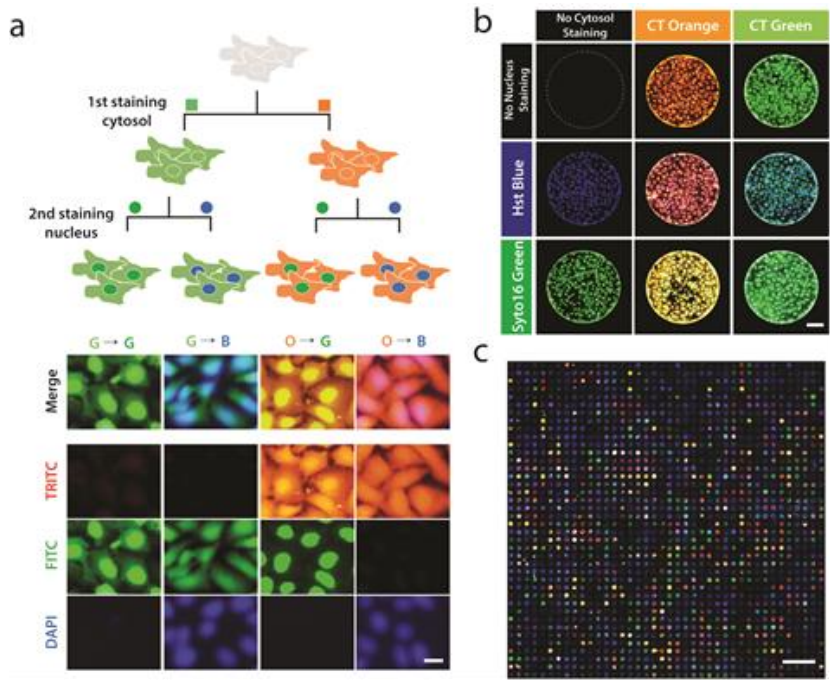


Figure 3.6 Sequential combinatorial cell staining for visual demonstration was demonstrated. (a) A schematic diagram for sequential staining procedure and its magnified image. Cell lines were firstly stained with cytosol staining dye -CellTracker$^{TM}$ green, orange and secondly stained with nucleus staining dye - Hoechst 33342(blue), Syto$^{TM}$ 16(green). (b) Every possible combination of sequential staining was presented. Nine combinations were observed including particles had not been loaded with staining dye intentionally. (c)

Sequential staining image of the whole chip. Scale bar: 5 mm. ( Reprinted from [21] )

Two-step sequential cell staining assay was demonstrated for the proof-of-concept of our sequential treatment assay

The detailed protocol for Sequential cell staining is as follows : To demonstrate heterogeneous sequential cell staining, 25 μL of 0.25 mM CellTracker™ (green and orange) staining dyes (Invitrogen) were loaded into the microparticles for cytosol staining. For the second staining, 25 μL of 0.05 mM Hoechest 33342 (blue) and SYTO™ 16 (green) staining dyes (Invitrogen) were loaded into the microparticles for nucleus staining. The incubation time for each staining step was 4 h.

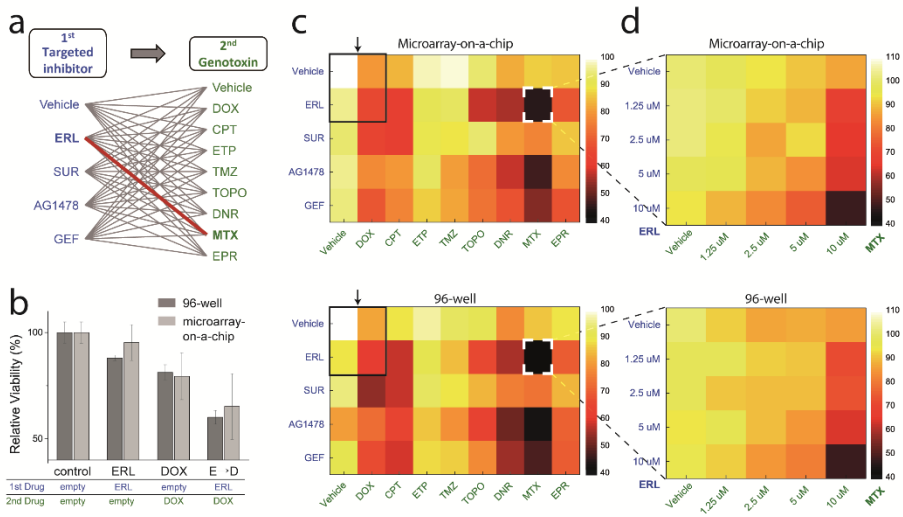


Figure 3.7 Large-scale sequential drug combination assay against BT-20, triple negative breast cancer, using heterogeneous drug-releasing hydrogel microarray. ) The list of screened sequential combinations. Library-to-library screening with targeted inhibitor treatment followed by genotoxin was implemented. b) Synergistic effect of sequential combinations. The results of erlotinib and doxorubicin are shown as representative examples. c) Sequential combination screening results from our platform using a microarray-on-a-chip and a conventional 96-well-based technique. Erlotinib followed by mitoxantrone was revealed as the most synergistic sequential pair (highlighted in white box) in the screened combination library. Black boxes indicate the data represented in (b). d) Dose–response matrix screening for

erlotinib followed by mitoxantrone. In all heat maps, the color of each spot represents the relative viability based on a negative control without any treatment (vehicle → vehicle). The color map on the right shows the percentage value of relative viability corresponding to the color. All viability data from the proposed platform and 96-well plate were within ±15% of each other. ( Reprinted from [21] )

I previously validated an availability of partipetting platform to screening of concurrent combinatorial drugs by controlling the design of the placement of microwell arrays on the assembly chip. However, the previous version of our platform could support only a single incubation step. In this work, I demonstrated a sequential combination assay with the concept of exchanging a drug-releasing hydrogel microarray-on-a-chip. This becomes available with the advantages of the 3D-align key on rigid plastic chips. For the proof-of-concept, a sequential cell staining assay was first demonstrated by using cytosol staining with green and orange CellTracker™ dyes followed by nucleus staining with blue Hoechst 33342 and green SYTO™ 16 nucleic acid staining dyes (Figure 5). Two drug-releasing hydrogel microarray-on-a-chips were combined sequentially on one cell chip. Hydrogel microarray-releasing cytosol-staining dyes and nucleus-staining dyes were placed on the first and second chip, respectively. It was confirmed that the

fluorescence images of cells were clearly distinguished depending on the combination of staining dyes treated sequentially (Figure 3.7). In total, nine combinations were possible using staining dyes, and I could find all of them from the images of microwells on the cell chip (Figure 3.7). For a large-scale experiment, a sequential combination staining experiment was conducted on a large-scale chip with 1,600 microwells (Figure 3.6). From these results, I validated that the sequential delivery of drugs to each isolated microwell is available in a scalable manner by exchanging a hydrogel microarray-on-a-chip.

For the cell viability assay, the detailed protocol is as follows : Calcein AM (Thermo Fisher Scientific) was used to stain live cells. Approximately 1 mg/mL Calcein AM solution was diluted in serum-free EMEM culture media at a 1:1000 ratio, and cells were incubated with the solution for 30 minutes. After PBS washing, fluorescence images of the microwells on a cell chip were obtained using a microscope setup with a motorized stage (Nikon Digital Sight DS-Ri1, Nikon C-LHGFI HG LAMP). A fluorescein isothiocyanate (FITC) channel filter (excitation 490 nm, emission 525 nm) and an exposure time of 200 ms for a 2x objective lens or 60 ms for 4x lens were used for image acquisition. Viability was decided by relative pixel intensity from the fluorescence image of a microwell area compared with non-drug treated microwells (control). For the average viability of each drug

combination, 10% of the upper and lower value data were excluded as outliers.

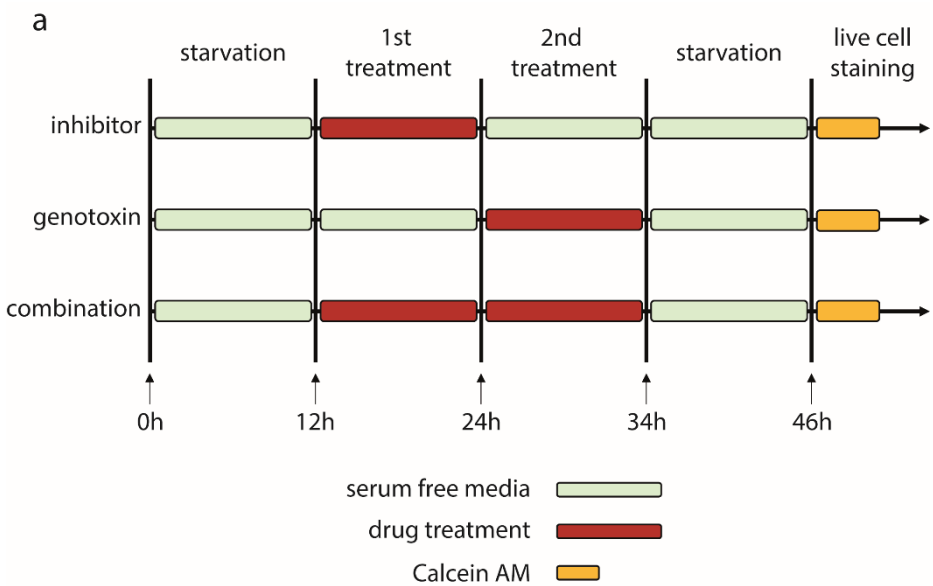


Figure 3.8. Timetable of sequential combination cytotoxicity assay.

Finally, I applied the proposed platform to conduct large-scale screening of the anticancer efficacy of sequential drug combinations (EGF receptor inhibitor followed by DNA damaging) agent against the triple-negative BT-20 cell line, which is particularly known as an aggressive form and has been widely being explored in clinical trials due to its poor prognosis (Figure 3.7). In the experiments, the final concentration of all drugs released from HYDROGEL MICROPARTICLE was adjusted to 10 μM, and each sequential drug was incubated for 12 hours with

inhibitory drugs and 10 hours with DNA damaging agent (time-table shown in Figure 3.8). For all combinations, the experimental results from 96-well plates and our platform had similar drug efficacies (Figure 3.7). The cytotoxicity of single drug therapies and sequential treatment from one combination, erlotinib and doxorubicin (indicated as a black box in Figure 3.7c), are represented in a bar graph (Figure 3.7b). From the screening results, erlotinib followed by mitoxantrone was revealed as the most effective sequential pair among total 45 combinations. The survival rate of cells treated with this pair was 44.46% in experiments using our platform and 40.63% in 96-well plate experiments. To evaluate the synergism of the combination, a dose-response matrix was also obtained using our platform (Figure 3.7d). All the results from the proposed platform were within ±15% of those obtained from a conventional approach, proving the feasibility of our platform for sequential drug combination assays.

In this study, I described large-scale screening platform to find effective sequential drug combinations. The delivery of encoded drug-laden microparticles using one-step pipetting and self-assembly of these microparticles to an array of microwells can replace thousands of pipetting operations. For a multi-step drug incubation, only a simple exchange of the hydrogel microarray-on-a-chip is required instead of repeating thousands of pipetting operations for every treatment step.

Furthermore, since our platform supports the screening of concurrent combinatorial drugs as well, this technique can apply to the various forms of combination screening. Such a significant decrease in workload gives hospitals and laboratories with limited resources the opportunity to perform large-scale, multi-step bioassays at an affordable cost and within a reasonable time. Regarding the required number of samples, only 200 cells per microwell were needed, and uniform seeding of 1,600 microwells was possible without a robotic pipette machine through the sealing film assisted seeding method. To make this platform usable by other researchers, I designed an easy-to-use platform by introducing 3-dimensional pillar/hole structures and a multipurpose holder for easy alignment.

It has not been long since researchers have understood that the underlying principle behind the effects of sequential combinations is the dynamics of signaling pathways. Therefore, there are many opportunities for new achievements, as our biological understanding of disease deepens. In addition, our platform for multi-step combinatorial screening can be potentially applied in other research fields, such as to include the differentiation and reprogramming of various cell types, to perform drug screening using cells transduced with various viral vectors, or to enable personalized drug scheduling using patient-derived cell lines. I expect that multi-step, large-scale screening using partipetting will be more accessible to researchers in a

wide range of fields, thereby broadening the applications of high-throughput, sequence-dependent combinatorial bioassays.

# Chapter 4 Drug Combination Assay on Patient-Derived Cells

In this chapter, I present another applicational study using patient-derived cells to find optimal drug screening result using in vitro drug screening platform. I demonstrated 2-combinatorial drug screening using patient-derived non-small-cell lung carcinoma (NSCLC) cells. First, I will briefly introduce the background and the motivation regarding the strategy of treating sequential drug combination. Second, I will present experimental design and relevant technical issue in the application of this platform to sequential drug combination assay. Then, I will explain technical issue and our engineering solution for handling the issue. Finally, I will present the result of drug combination assay using patient-derived cells.

## 4.1 Background : Simultaneous Combination Treatment using Patient-Derived Cells

Identification of somatic genetic modifications in tumors may dictate the selection of effective targeted therapies. Advances in sequencing technology and target identification have had a major impact, but only a handful of cancer patients are treated based on the identification of specific gene mutations. In addition, the response to targeted therapies among genetically defined patients is heterogeneous. Matching gene mutations and therapeutics is currently limited by an incomplete understanding of the relationship between tumor genotype and drug sensitivity. In addition, opportunities presented by rare, exceptional respondents in unselected patients are not utilized by current patient selection strategies.

At current level of understanding of molecular approach of clinical treatment, drug combination screening using ex vivo culture model can be an alternative approach for finding optimal drug pair for those who have acquired resistance of cancer drug for targeted therapy.

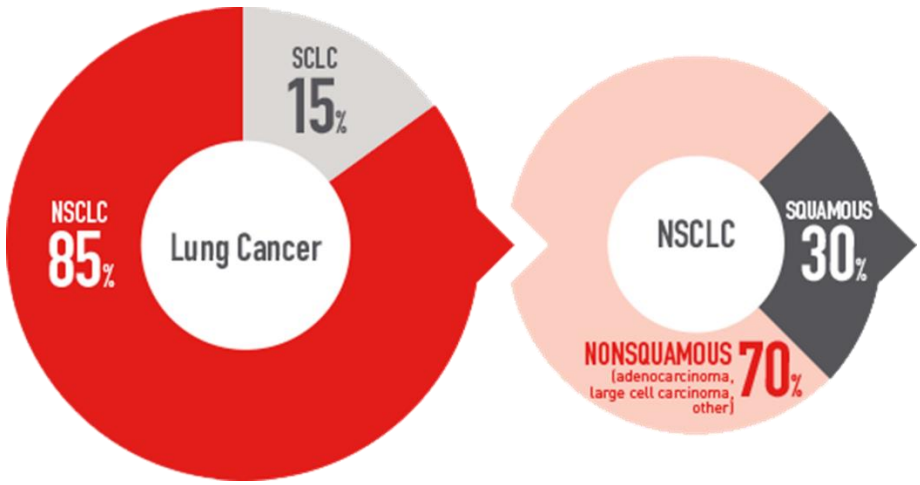


Figure 4.1 Statistics with Lung Cancer with a focus on NSCLC Non-Small Cell Lungs Cancer patients, which account for the largest portion of Lung Cancer.[31]

Especially in NSCLC, non-small cell lung cancer, lung cancer is the second most common cancer in both men and women (2020, USA). It accounts for 85% of lung cancer patients (Figure 4.1). According to the American Cancer Society, lung cancer has a poor prognosis. More than half of people diagnosed with lung cancer die within 1 year of diagnosis and the 5-year survival rate is less than 19%. NSCLC accounts for the majority of all lung cancer cases (Figure 4.2). Depending on the staging of lung cancer, patients may receive certain treatments ranging from surgery to radiation, chemotherapy and targeted therapy. As genetic and biomarker tests progressed, specific mutations were identified for better targeted treatment of

individual patients. However, many patients in stages 3 and 4 have acquired drug resistance of previously prescribed drugs for targeted therapies such as EGFR, ALK and ROS as major driving mutations. That means they have a path that is not well regulated by the tumor resistance mechanism. About 40% of newly diagnosed lung cancer patients have stage 4 (Figure 4.2), the goal of treating this patient is to improve survival and reduce disease-related side effects. For stage IV NSCLC, cytotoxic combination chemotherapy is a primary therapy that can be affected by histology, genetic factors, etc. The results of four large-scale, multicenter, randomized clinical trials that studied the agent with platinum or carboplatin produced similar results. From these studies, the results showed that monotherapy showed no significant superiority over other combinations. The specific combination depends on types and frequencies of toxic effects and should be determined on an individual basis.[31,32]

| NSCLC Stage | Distribution | NSCLC Stage | 1-Year Survival | 5-Year Survival |
|---|---|---|---|---|
| I | 13% - 24% | IA<br>IB | 91%<br>72% | 50%<br>43% |
| II | 5% - 10% | IIA<br>IIB | 79%<br>59% | 36%<br>25% |
| III | 31% - 44% | IIIA<br>IIIB | 50%<br>37%<br>32% | 19%<br>7% |
| IV | 32% - 39% | IV | 20% | 2% |

Figure 4.2. NSCLC distribution by stage and associated survival rates

## 4.2 Improvement of Platform for facilitating translational study

Before we conducted applicational study, we slightly modified our platform by integrating Particle chip and Transfer Chip into single PS-PDMS double layered chip for the efficiency of assembly and ease of use for end-user. It would enable collaborators to access to our platform more easily with better user convenience.

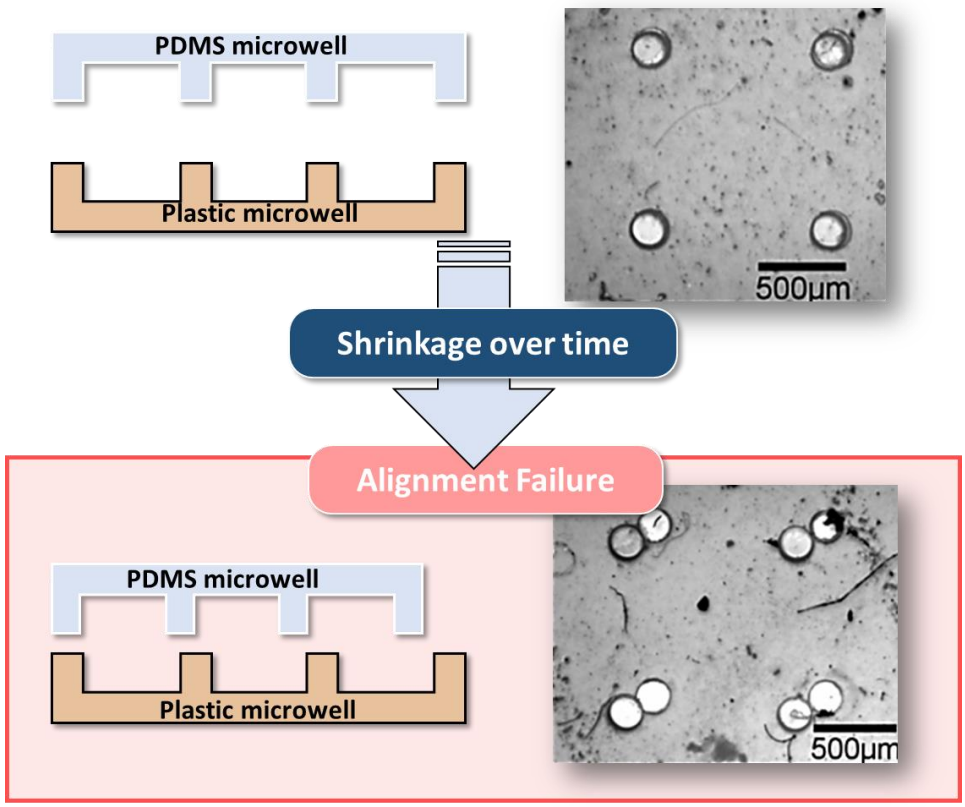


Figure 4.3 A schematic illustration in the integration of PS-PDMS chip for preparation of drug-laden hydrogel microarray.

Thus, we had a collaboration with Yonsei severance hospital for drug screening for functional drug testing using patient-derived cell lines. Before we screen among selected drug panel of drugs for targeted therapy of NSCLC. Before we had a co-working for translational research. We had an issue of the integration of particle chip and transfer chip. The integration of PDMS-PS chip could solve the issue of

shrinkage of PDMS microwell when it is solely used alone in alignment of particle assembled chip and cell chip, which could lead to the failure of bioassay. Additionally, it could increase the user-friendliness because when only Polystyrene-based plastic chip was used, the overall

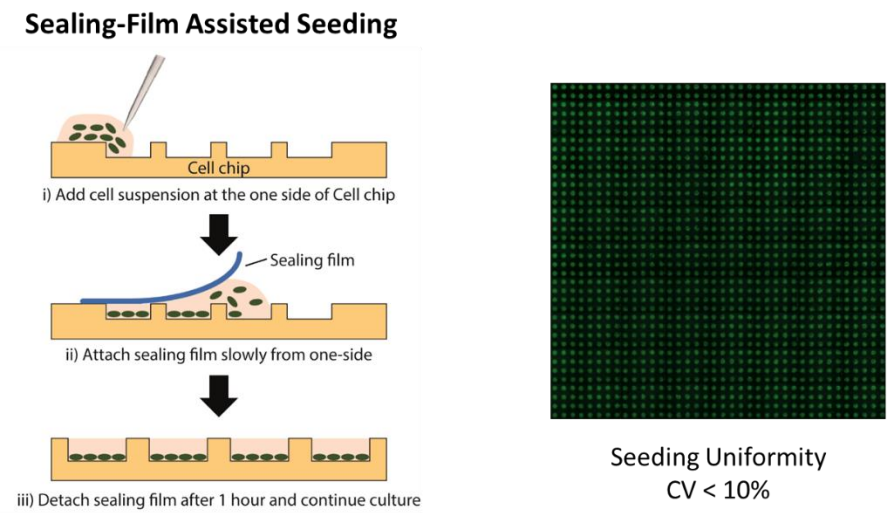


Figure 4.4 Fabrication Process of PS-PDMS double layered soft lithography for alignment registration issue.

A new method of sealing film-assisted seeding cells has been invented to reduce cell suspension of dead cell volume in cell seeding. Since we thought that the drug screening platform requires fewer cells in the screening process, the clinical value will be maximized by drastically reducing the time to

prescribe personalized drugs.

## 4.3 Study Design for small-volume drug combinatorial screening with NSCLC patient derived cell

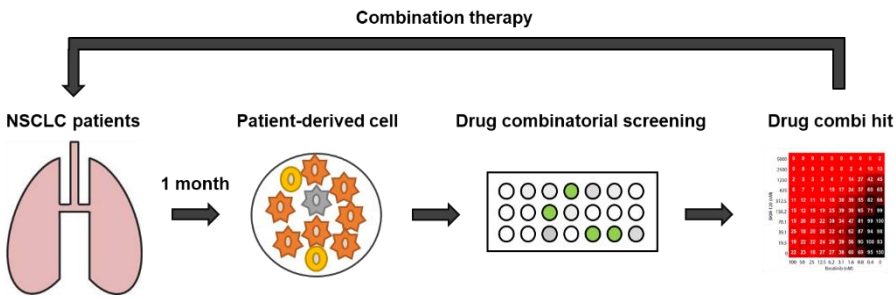


Figure 4.5 A schematic illustration of study design on drug combinatorial screening using NSCLC patient-derived cell line.

Combination drug therapy has been shown to increase the efficacy and reduce the dose of individual drugs because each drug acts on different, often complementary, targets and signaling pathways. For instance, combination treatment of Erlotinib (EGFR tyrosine kinase inhibitor) and ramucirumab (VEGFR2 antagonist) improved progression-free survival in EGFR-mutated metastatic non-small-cell lung cancer NSCLC) patients as a result of the blockade of both the EGFR and VEGF pathways. Importantly, reduced or no unexpected toxicities resulted. This combination therapy

is currently in Phase III clinical trials, there are a number of other combination therapy trials underway in NSCLC patients.

In addition to the clinical advances, high throughput screening of drug combinations was carried out to identify a synergistic combination. An interesting aspect of this is combining multiple drug combination screening with patient-derived cell lines.

| | Target | Drug |
|---|---|---|
| Main driver mutation | ALK | Crizotinib |
| | | Lorlatinib |
| | EGFR | Ceritinib |
| | | Gefitinib |
| | | Afatinib |
| | | Osimertinib |
| Drug-resistant mutation | pan-HER | Dacomitinib |
| | MEK | Trametinib |
| | mTOR | Everolimus |
| | SRC, c-Kit | Dasatinib |
| | HSP | Tanespimycin |

Table 1 List of drug library for NSCLC cancer patients. These drugs were loaded onto microparticles as their target concentration to be 5 μM.

Drug library to be screen for finding optimal drug pair was selected with two group. The first group can be explained in terms of main driver mutation for NSCLC. And

the second group is anticancer drug for NSCLC as another target of molecular pathway for inducing drug-resistant mutant. (Table 1)

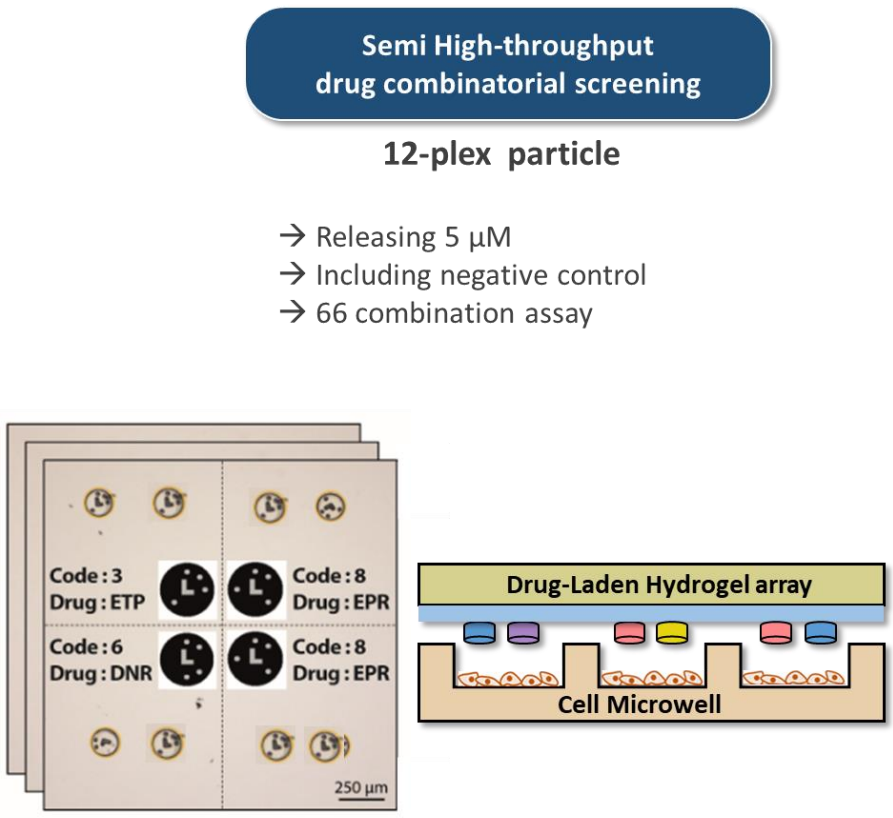


Figure 4.6 Preparation of particle chip for 2-combinatorial drug testing based on the constructed drug library including drug types of inhibiting main driver mutation and drug-resistant mutation for lung cancer patient.

## 4.4 Assay Result

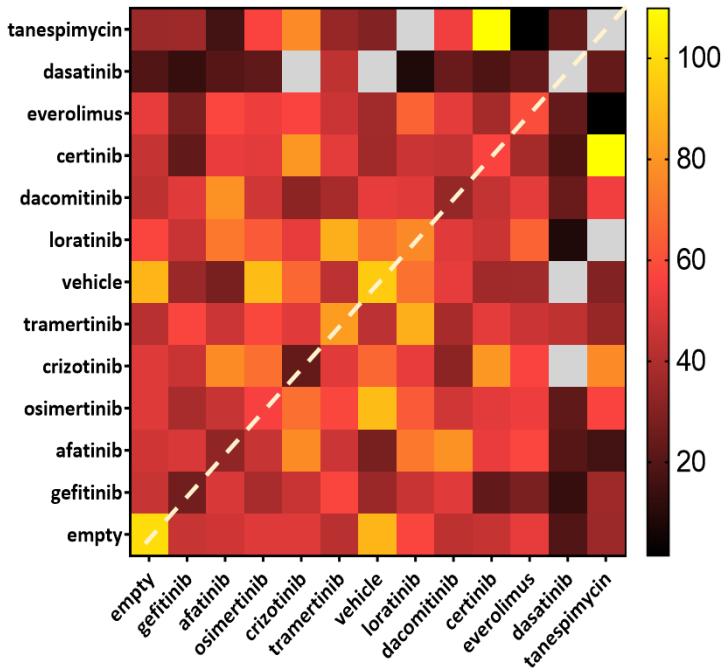


Figure 4.7 A heatmap analysis using NSCLC patient-derived cells.

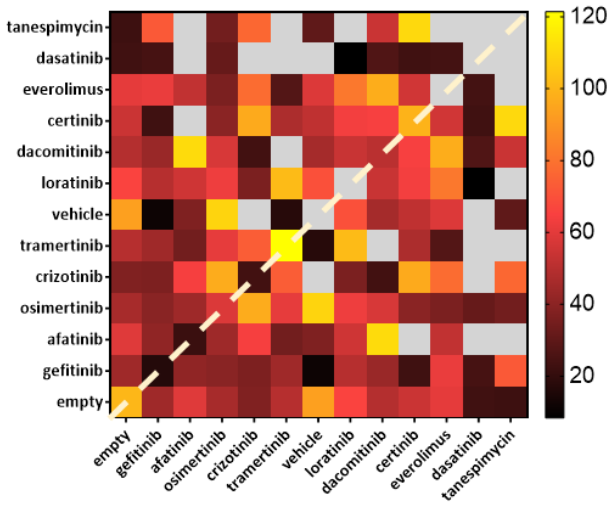


Figure 4.8. A heatmap analysis using NSCLC patient-derived cells.

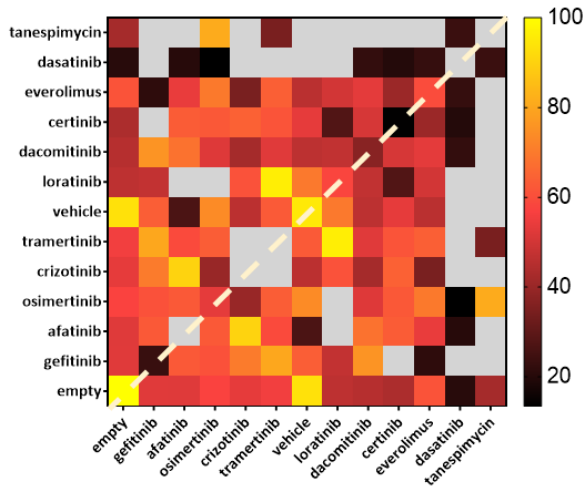


Figure 4.9. A heatmap analysis using NSCLC patient-derived cells.

The patient-derived cell line had been established using the tumor biopsy sample from the NSCLC patients who had acquired resistance of mainly EGFR mutation as main driver mutation and another drug-resistant mutation. The sample was screened on our platform for 3 days according to the protocol shown in the figure 4.6.

The result was that although some combinations were not included in this heatmap from the viability assay result, some notable combination was identified in the initial screening.

# Chapter 5 Development of platform for 3D culture model

In this chapter, I demonstrate engineering Cell Chip that enable 3D cell culture assisted by Matrigel scaffold. First, I introduce the background about the necessity of 3D cell culture model in in vitro drug screening platform. Second, I describe the technical difficulty and solution in translating proposed in vitro drug testing platform from 2D monolayer cell culture-based platform to 3D cell culture platform. Then, as a validation for 3d spheroid culture on our platform, I visualized 3d cell culture model using Hoechst nucleus counterstaining dye and CellTracker™ for cytosol staining. Lastly, I analyzed cost comparison of Matrigel™ usage between the proposed platform and conventional well plate-based approach.

## 5.1 3D culturable platform

Conventional two-dimensional (2D) monolayer cell cultures have been used traditionally, but such models have had limited success in translating to complex and heterogeneous in vivo environments and thus resulting in poor predictors of clinical trial outcomes[33,34]. To overcome these drawbacks, three-dimensional (3D) cell culture methods that better mimic in vivo environments have been applied to drug toxicity testing and have provided better precision in drug discovery

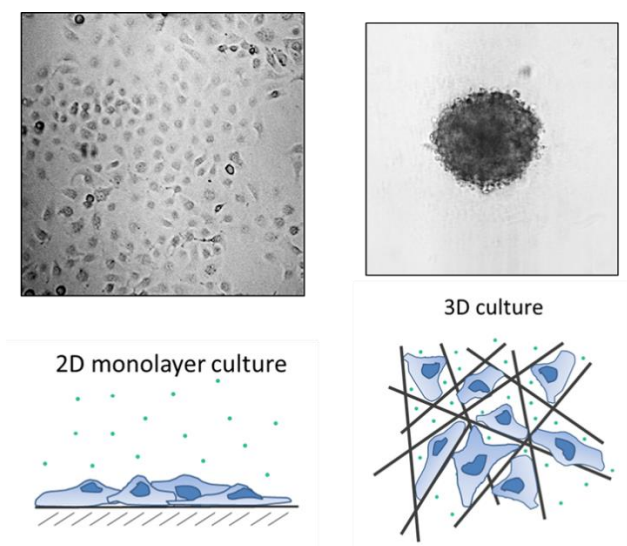


Figure 5.1 In vitro 2D monolayer culture have limitations in reflecting cancer cell's status in vivo

Over the past 20 years, 3D cell culture has been chosen as a model that more closely represents the situation in vivo. Tumor spheroids, also called organotypic multicellular spheroids, and organoids are examples of the most commonly used 3D cell models in oncology. Tumor spheroids are solid spherical aggregates of tumor cells that can be expressed as cancer cell lines or patient-derived cancer cells derived from autologous organization of single cells. In contrast to spheroids, tumor organoids are formed by mechanically or enzymatically disintegrating the original tumor tissue into small pieces and then culturing these tumor pieces in an extracellular matrix network such as Matrigel (Figure 5.1, Figure 5.2) (Figure 5.1, Figure 5.2)[33,35–40]

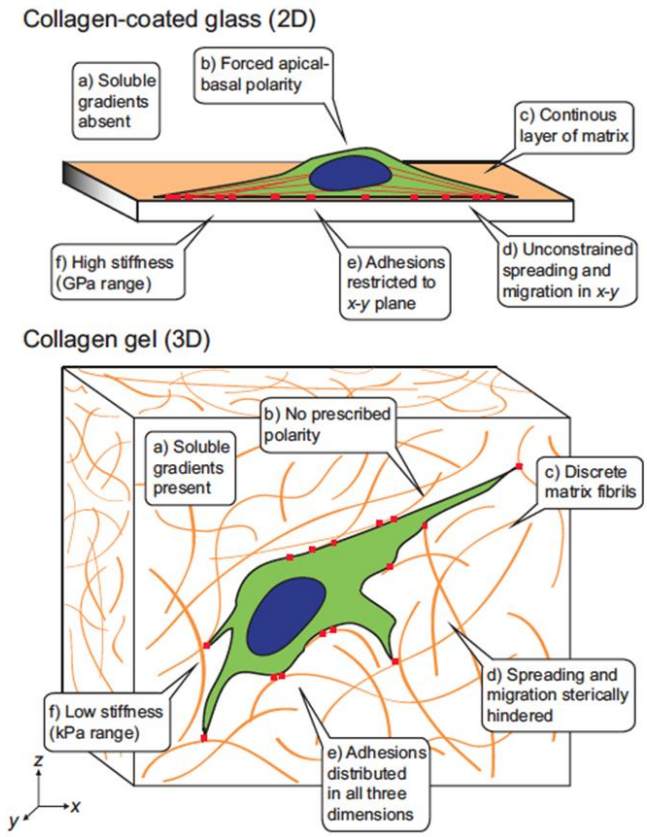


Figure 5.2 A Feature comparison between 2D and 3D Cell Culture

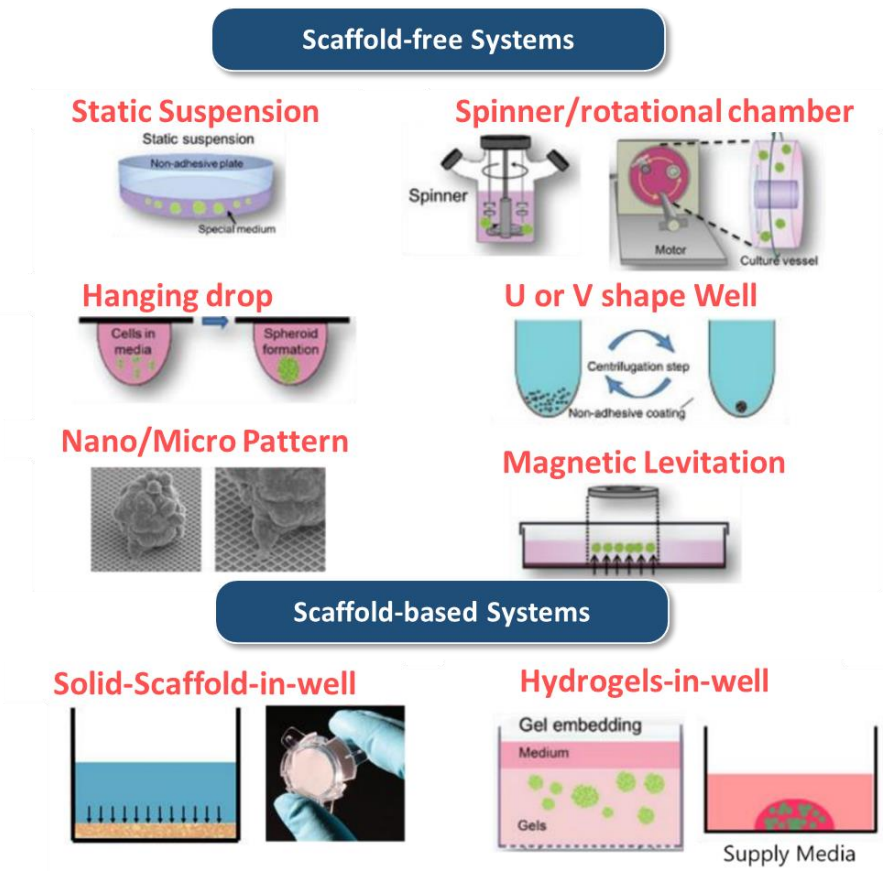


Figure 5.3 Methods available for formation of spheroid model.[41,42]

The suspension culture method was invented to isolate and culture neural stem cells[43]. Subsequently it became a widely used 3D cell culture method. The main features of this method are a serum-free and artificially low adhesion cell growth microenvironment (Figure 5.3). as another culturing method, device-assisted culture, it is an improvement of the static suspension

culture, depending on several biological devices, including magnetic levitation[44], spinner or rotational bioreactors[45] and microfluidics devices. The main feature of these bioreactors is to prevent tumor cells from attaching or stop their movement so that they can grow into ellipsoids. In addition, the microcarrier or microcapsules are often used to increase the efficiency of cell growth were combined to improve the protection of the mobile cell.

For the scaffold assisted 3d cell culture method, a gel insertion culture method using collagen, alginate and Matrigel. In particular, Matrigel is derived from the basement membrane protein from Engelbreth-Holm-Swarm mouse tumor cells, which includes collagen IV, laminin, multiple cytokines and growth factors. It has wider commercial applications in numerous tumor cell experiments, including 3D culture and tumor invasive models.[45]

In general, the procedures for preparing the scaffolds fall into one of two major categories: 1, natural polymers derived from natural polymer materials, including collagen, chitosan, glycosaminoglycans (mainly hyaluronic acid), fibroin, agarose, alginate, and starch (mainly used as additives); and 2, synthetic polymers, containing polyglycolic acid, polylactic acid, polyorthoester and their copolymers or blends, as well as the aliphatic polyester polycaprolactone. While natural polymers have improved

biocompatibility and toxicity, artificial synthetic polymers have improved versatility, reproducibility, workability, and in most cases are easier to process than the former, but not bioactive. The processing technique of scaffolding preparation is much more complicated than gel insertion.

## 5.2 Development of 3D culture platform based Matrigel scaffold.

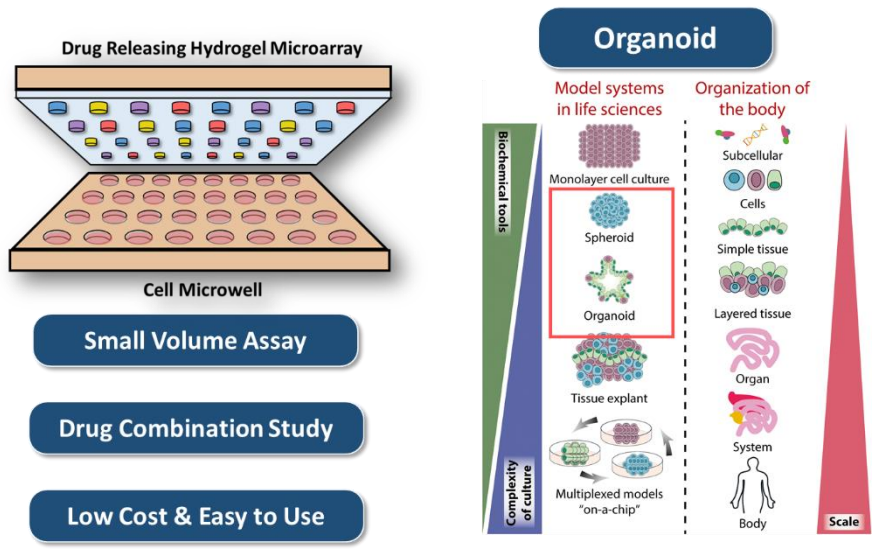


Figure 5.4 Current advantage of the platform and its necessity for a platform that is capable of 3D spheroid, organoid culture

As I explained the strength of our platform as stated in the left of the figure 5.4. In

vitro drug screening platform using drug releasing hydrogel microarray technology is capable of small-volume assay, high-throughput drug combination study and low cost and easy-to-use screening process. However, as the trend of 3d culture in drug screening to better mimic in vivo status of human. I also investigated 3d culture method to apply 3d culture method to our cell chip.

Among many methods of 3d formation of spheroids and organoids, I decided to adopt 3d scaffold-assisted culture method.

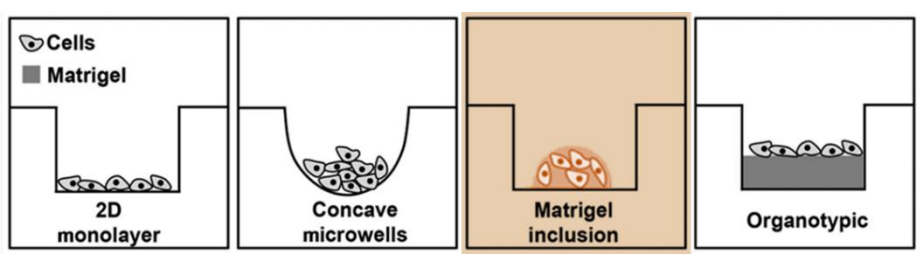


Figure 5.5 Description of basic classification for in vitro culture methods in generating 2D monolayer culture, spheroid, and organoid.

**Staining Result of 3D spheroid culture on our platform.**

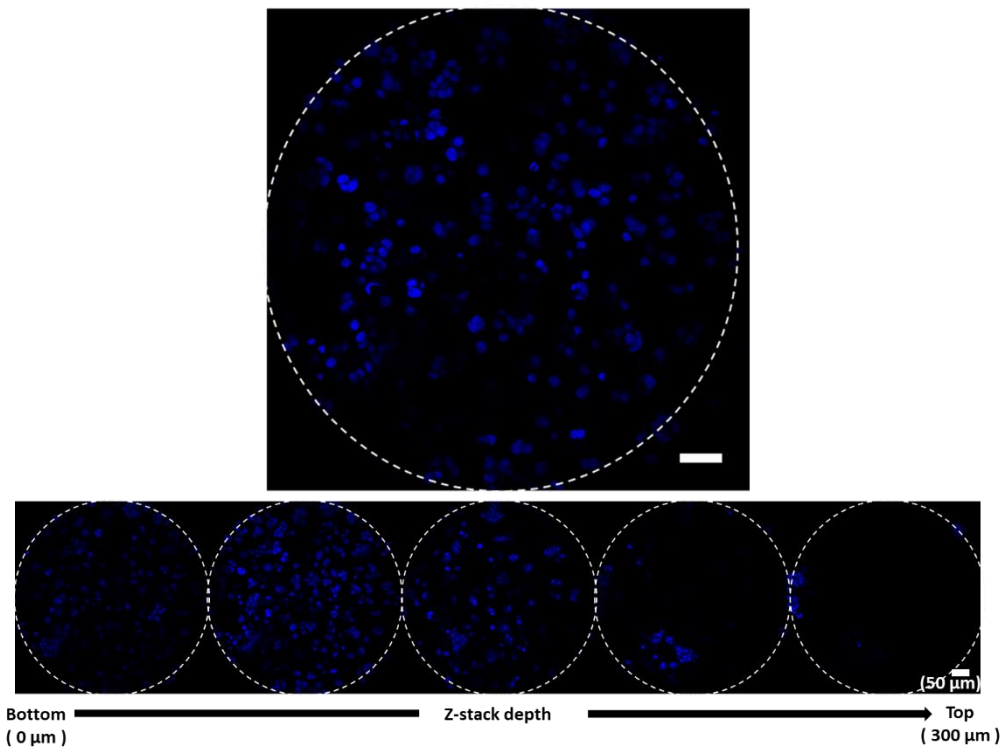


Figure 5.6 Z-stack images of 3d distribution of spheroids on Cell Chip.

Figure 5.7 shows the distribution of MCF-7 cell line in the spheroids along z-axis of the inside of the microwell. Z-sectioned fluorescence image was roughly taken from 0 micrometer, the bottom of the microwell, to 300 micrometers, almost the top of the microwell. For visualization, the nuclei of the MCF-7 cells were imaged with DAPI filter after stained with Hoechst 33482 and the cytosol of the cells were imaged with FITC filter after stained

with CellTracker Green.

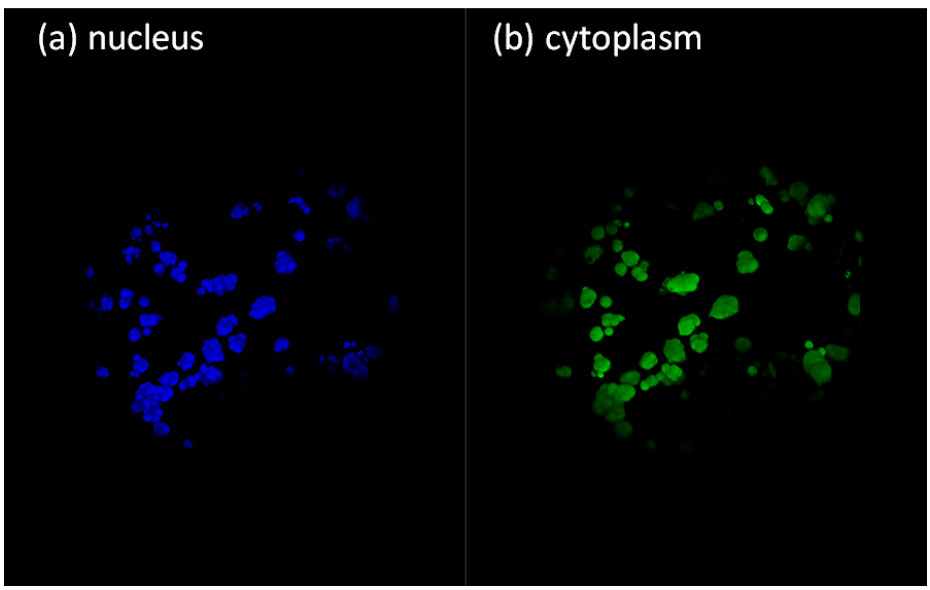


Figure 5.7. The 3d reconstruction images of confocal z-stacks of MCF-7 spheroids. Image acquisition was done by Fluorescence Confocal Microscopy. Hoechst 33342 for nuclei staining and CellTracker$^{TM}$ Green dye for cytoplasm staining were used. ( 20x Magnification )

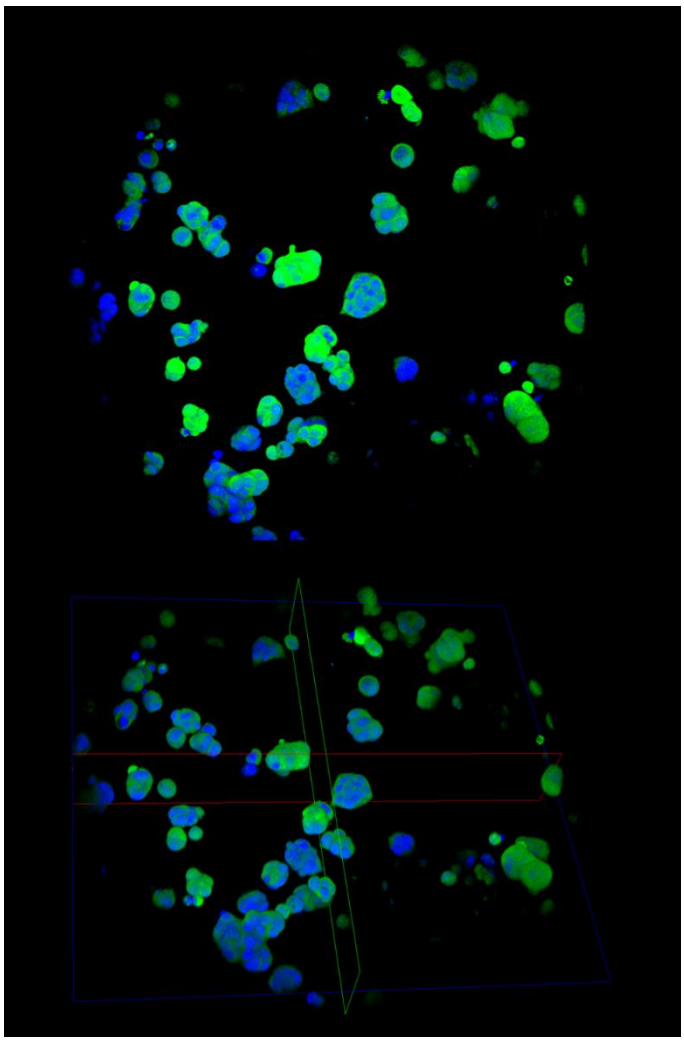

Figure 5.8 3D reconstruction image of confocal z-stacks of MCF-7 spheroids inside one microwell at different viewing angles. Image acquisition was done by Fluorescence Confocal Microscopy.

As shown in the Figure 5.8, 5.9, 3d imaging of Matrigel-embedded spheroids on our platform was obtained using confocal microscopy for the visual demonstration of the status of cell culture on microwell.

The detailed staining protocol is as follows : First, CellTracker Green : x1000 dilution of stock. Solution for 30min at 37 deg. And then, 4% Paraformaldehyde(PFA) fixation for 10 min at R.T. Then, Hoechst for Nucleus staining: stock sol. X2,000 dilution (1% BSA/PBS) for 20min, 37 deg. Lastly, Fluorescence Imaging was imaged by confocal microscopy (Leica, SP8 X, 20x magnification)

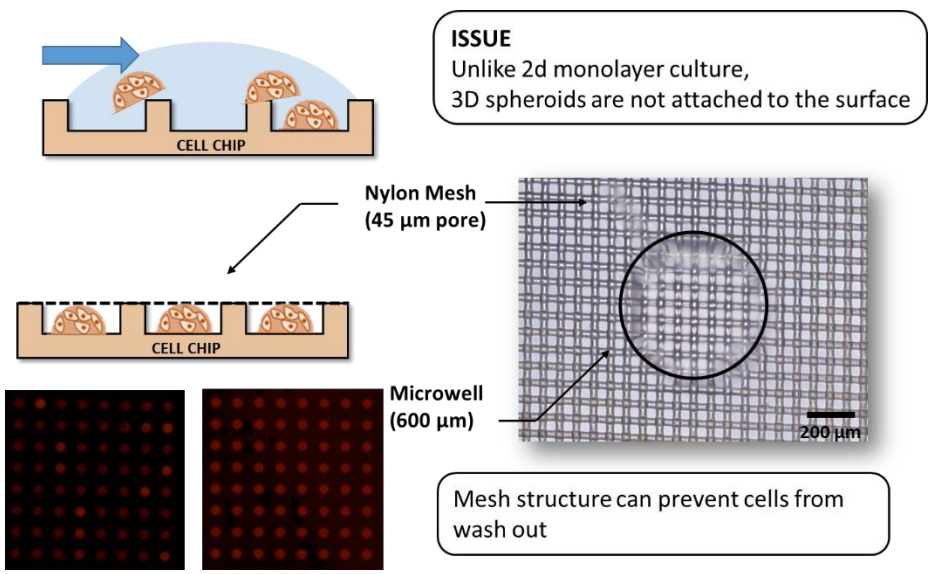


Figure 5.9. Retention of 3D spheroids from microwell in media exchange can be achieved by using Nylon mesh Structure.

As cancer cells are formed in the microwell assisted by gel scaffold, the spheroids are not in the status of attached to the surface. Thus, it can be washed away in case of media exchange or suctioning. Specifically, in our platform.

## 5.3 Advantage over conventional 3D culture-based drug testing platform.

| | Platform in this thesis (400 microwell) | 96-well plate (400 well) |
|---|---|---|
| Volume of Microwell (μL) | 0.1 | 100 |
| Matrigel Volume Per well((μL) | 0.5 | 50 |
| Total Matrigel Usage ((μL)) | $1.5 \times 10^2$ | $2.0 \times 10^4$ |
| Cost | $ 6 | $ 800 |

Figure 5.10. Cost analysis of the use of Matrigel™ volume for 400 combinatorial drug testing.

In many applicational area using organoid, many groups researching organoid development for drug discovery, development biology are widely using Matrigel for their scaffold for 3D culture. Our platform can now become 3d culturable platform. As with many strengths in our platform, one more notable

competitiveness exists in our platform in terms of cost reduction. After we have done cost analysis of the use of Matrigel volume for 400 combinatorial drug testing as the single unit of the small chip in our platform.

# Chapter 6 Conclusion

In this dissertation, I presented miniaturized high-throughput drug screening biochip for small-volume bioassay in a high-throughput way. In this study, I construct a heterogeneous drug-loaded microparticle library by fabricating encoded photocurable polymer particle that has individually identifiable codes to track loaded drug. and I load various drug molecules, which I want to test to target cells, into each coded microparticle. Then, I developed to produce heterogeneous drug-laden microparticle arrays through simple self-assembly without the need for a microarray spotter or dispensing machine for generating microarray. I also have developed cell seeding method of seeding small-volume samples into the microwell-based cell chip. By utilizing the drug-laden microparticle hydrogel array and microwell-based cell chip technology, hundreds to thousands of different assays can be done at once with just a small number of samples and low cost. Through the implemented platform, the anti-cancer drug sequential combination screening was conducted on the triple-negative breast cooler (TNBC) cells, which are generally known to be difficult to

treat due to lack of known drug target, and the results of screening were analyzed by establishing a library of drugs in the EGFR inhibitory type and drugs in the genotoxin type. In addition, another study was conducted to find optimal drug combinations using patient-derived cells derived from tumors in patients with non-small cell lung cancer that have obtained acquired resistance. Finally, as the growing need for three-dimensional culture, such as spheroid and organoid for having a similar response to in vivo drug testing, it was also developed that microwell-based cell chip that is capable of 3D culture with low-cost and small-volume of cells.

However, though high-throughput drug screening technology for this purpose is of the utmost importance in saving lives, there were many limitations to its wide use in many hospitals. The existing high-throughput drug combination screening technology consumes a large number of samples and consumes a considerable amount of expensive reagents. In addition, expensive automated liquid handlers, which were essential for exploring thousands of different pipetting, were not easy to introduce except for large-sized pharmaceutical companies and research institutes, which limited access to technology.

The miniaturized in vitro anticancer drug screening platform presented in this study has the following significance. An easy-to-use technique that can be applied

to a small number of patient cells or samples, which can dramatically reduce the use of conventional expensive equipment, reagents. The proposed technology in this study can be applied to a variety of academic studies previously inaccessible to high-throughput screening due to the high cost of reagents, the high price of equipment, or the limited amount of samples in conventional drug screening. and this platform can also dramatically increase access to clinical research in hospitals for personalized treatments. Additionally, I believe that the applicability of this platform can maximized for personalized cancer patient care if it is used in a relatively small and medium-sized clinical research environment by the combined use of various rare samples such as patient-derived cells or patient-derived organoids.

# Bibliography

[1] O. M. Kutova, E. L. Guryev, E. A. Sokolova, R. Alzeibak, I. V. Balalaeva, *Cancers* **2019**, *11*, 68.

[2] L. Da-Yong, L. Ting-Ren, W. Hong-Ying, *Clin Exp Pharmacol* **2014**, *04*, DOI 10.4172/2161-1459.1000153.

[3] C. L. Tourneau, E. Borcoman, M. Kamal, *Nat Med* **2019**, *25*, 711.

[4] I. V. Hinkson, T. M. Davidsen, J. D. Klemm, I. Chandramouliswaran, A. R. Kerlavage, W. A. Kibbe, *Frontiers Cell Dev Biology* **2017**, *5*, 83.

[5] V. Malhotra, M. C. Perry, *Cancer Biol Ther* **2003**, *2*, 1.

[6] R. Dienstmann, I. S. Jang, B. Bot, S. Friend, J. Guinney, *Cancer Discov* **2015**, *5*, 118.

[7] Y. Yuan, E. M. V. Allen, L. Omberg, N. Wagle, A. Amin-Mansour, A. Sokolov, L. A. Byers, Y. Xu, K. R. Hess, L. Diao, L. Han, X. Huang, M. S. Lawrence, J. N. Weinstein, J. M. Stuart, G. B. Mills, L. A.

Garraway, A. A. Margolin, G. Getz, H. Liang, *Nat Biotechnol* **2014**, *32*, 644.

[8] E. M. V. Allen, N. Wagle, P. Stojanov, D. L. Perrin, K. Cibulskis, S. Marlow, J. Jane-Valbuena, D. C. Friedrich, G. Kryukov, S. L. Carter, A. McKenna, A. Sivachenko, M. Rosenberg, A. Kiezun, D. Voet, M. Lawrence, L. T. Lichtenstein, J. G. Gentry, F. W. Huang, J. Fostel, D. Farlow, D. Barbie, L. Gandhi, E. S. Lander, S. W. Gray, S. Joffe, P. Janne, J. Garber, L. MacConaill, N. Lindeman, B. Rollins, P. Kantoff, S. A. Fisher, S. Gabriel, G. Getz, L. A. Garraway, *Nat Med* **2014**, *20*, 682.

[9] C. Pauli, B. D. Hopkins, D. Prandi, R. Shaw, T. Fedrizzi, A. Sboner, V. Sailer, M. Augello, L. Puca, R. Rosati, T. J. McNary, Y. Churakova, C. Cheung, J. Triscott, D. Pisapia, R. Rao, J. M. Mosquera, B. Robinson, B. M. Faltas, B. E. Emerling, V. K. Gadi, B. Bernard, O. Elemento, H. Beltran, F. Demichelis, C. J. Kemp, C. Grandori, L. C. Cantley, M. A. Rubin, *Cancer Discov* **2017**, *7*, 462.

[10] B. Vogelstein, N. Papadopoulos, V. Velculescu, S. Zhou, L. Diaz, K. Kinzler, *Science* **2013**, *339*, 1546.

[11] S. J. Kwon, D. W. Lee, D. A. Shah, B. Ku, S. Y. Jeon, K. Solanki, J. D. Ryan, D. S. Clark, J. S. Dordick, M.-Y. Lee, *Nat Commun* **2014**, *5*, ncomms4739.

[12] F. Eduati, R. Utharala, D. Madhavan, U. P. Neumann, T. Longerich, T. Cramer, J. Saez-Rodriguez, C. A. Merten, *Nat Commun* **2018**, *9*, 2434.

[13] T. Satoh, S. Sugiura, K. Shin, R. Onuki-Nagasaki, S. Ishida, K. Kikuchi, M. Kakiki, T. Kanamori, *Lab Chip* **2017**, *18*, 115.

[14] T. Tronser, K. Demir, M. Reischl, M. Bastmeyer, P. A. Levkin, *Lab Chip* **2018**, *18*, 2257.

[15] M. R. Carstens, R. C. Fisher, A. P. Acharya, E. A. Butterworth, E. Scott, E. H. Huang, B. G. Keselowsky, *Proc National Acad Sci* **2015**, *112*, 8732.

[16] Y. Sun, X. Chen, X. Zhou, J. Zhu, Y. Yu, *Lab Chip* **2015**, *15*, 2429.

[17] G. Svedberg, Y. Jeong, H. Na, J. Jang, P. Nilsson, S. Kwon, J. Gantelius, H. A. Svahn, *Lab Chip* **2017**, *17*, 549.

[18] S. Han, H. J. Bae, S. D. Kim, W. Park, S. Kwon, *Lab Chip* **2017**, *17*, 2435.

[19] H. Lee, J. Kim, H. Kim, J. Kim, S. Kwon, *Nat Mater* **2010**, *9*, 745.

[20] D. Y. Oh, H. Na, S. W. Song, J. Kim, H. In, A. C. Lee, Y. Jeong, D. Lee, J. Jang, S. Kwon, *Biomicrofluidics* **2018**, *12*, 031101.

[21] S. W. Song, S. D. Kim, D. Y. Oh, Y. Lee, A. C. Lee, Y. Jeong, H. J. Bae, D. Lee, S. Lee, J. Kim, S. Kwon, *Adv Sci* **2019**, *6*, 1970014.

[22] Y. Song, Y. Jeong, T. Kwon, D. Lee, D. Oh, T.-J. Park, J. Kim, J. Kim, S. Kwon, *Lab on a Chip* **2016**, *17*, 429.

[23] S. W. Song, S. D. Kim, D. Y. Oh, Y. Lee, A. C. Lee, Y. Jeong, H. J. Bae, D. Lee, S. Lee, J. Kim, S. Kwon, *Adv Sci* **2019**, *6*, 1801380.

[24] S. Chung, J. Kim, D. Oh, Y. Song, S. Lee, S. Min, S. Kwon, *Nature Communications* **2014**, *5*, 3468.

[25] S. Koplev, J. Longden, J. Ferkinghoff-Borg, M. Bjerregård, T. R. Cox, J. T. Erler, J. T. Pedersen, F. Voellmy, M. Sommer, R. Linding, *Cell Reports* **2017**, *20*, 2784.

[26] S. Chen, W. Forrester, G. Lahav, *Science* **2016**, *351*, 1204.

[27] D. Miles, G. von Minckwitz, A. D. Seidman, *Oncol* **2003**, *8*, 124.

[28] M. J. Lee, Y. S. Albert, A. K. Gardino, A. Heijink, P. K. Sorger, G. MacBeath, M. B. Yaffe, *Cell* **2012**, *149*.

[29] J. S. Lim, *Osteoporos Sarcopenia* **2018**, *4*, S6.

[30] F. Cardoso, P. L. Bedard, E. P. Winer, O. Pagani, E. Senkus-Konefka, L. J. Fallowfield, S. Kyriakides, A. Costa, T. Cufer, K. S. Albain, E.-M. T. Force, *J Natl Cancer I* **2009**, *101*, 1174.

[31] C. Zappa, S. A. Mousa, *Transl Lung Cancer Res* **2016**, *5*, 288.

[32] D. P. Kodack, A. F. Farago, A. Dastur, M. A. Held, L. Dardaei, L. Friboulet, F. von Flotow, L. J. Damon, D. Lee, M. Parks, R. Dicecca, M. Greenberg, K. E. Kattermann, A. K. Riley, F. J. Fintelmann, C. Rizzo, Z. Piotrowska, A. T. Shaw, J. F. Gainor, L. V. Sequist, M. J. Niederst, J. A. Engelman, C. H. Benes, *Cell Reports* **2017**, *21*, 3298.

[33] L. Zhao, J. Xiu, Y. Liu, T. Zhang, W. Pan, X. Zheng, X. Zhang, *Sci Rep-uk* **2019**, *9*, 19717.

[34] C.-T. Kuo, J.-Y. Wang, Y.-F. Lin, A. M. Wo, B. P. C. Chen, H. Lee, *Sci Rep-uk* **2017**, *7*, 4363.

[35] E. J. Vrij, S. Espinoza, M. Heilig, A. Kolew, M. Schneider, C. A. van Blitterswijk, R. K. Truckenmüller, N. C. Rivron, *Lab Chip* **2016**, *16*, 734.

[36] J. Casey, X. Yue, T. D. Nguyen, A. Acun, V. R. Zellmer, S. Zhang, P. Zorlutuna, *Biomed Mater* **2017**, *12*, 025009.

[37] K. ZEEBERG, R. A. CARDONE, M. R. GRECO, M. SACCOMANO, A. NØHR-NIELSEN, F. ALVES, S. F. PEDERSEN, S. J. RESHKIN, *Int J Oncol* **2016**, *49*, 243.

[38] K. Schneeberger, B. Spee, P. Costa, N. Sachs, H. Clevers, J. Malda, *Biofabrication* **2017**, *9*, DOI 10.1088/1758-5090/aa6121.

[39] J. M. Lee, D. Y. Park, L. Yang, E.-J. Kim, C. D. Ahrberg, K.-B. Lee, B. G. Chung, *Sci Rep-uk* **2018**, *8*, 17145.

[40] D. Barata, C. van Blitterswijk, P. Habibovic, *Acta Biomaterialia* **2016**, *34*, 1.

[41] D. Lv, Z. Hu, L. Lu, H. Lu, X. Xu, *Oncol Lett* **2017**, *14*, 6999.

[42] Y.-C. Tung, A. Y. Hsiao, S. G. Allen, Y. Torisawa, M. Ho, S. Takayama, *Analyst* **2011**, *136*, 473.

[43] B. Reynolds, S. Weiss, *Science* **1992**, *255*, 1707.

[44] G. R. Souza, J. R. Molina, R. M. Raphael, M. G. Ozawa, D. J. Stark, C. S. Levin, L. F. Bronk, J. S. Ananta, J. Mandelin, M.-M. Georgescu, J. A. Bankson, J. G. Gelovani, T. C. Killian, W. Arap, R. Pasqualini, *Nat Nanotechnol* **2010**, *5*, 291.

[45] B. Marrero, J. L. Messina, R. Heller, *Vitro Cell Dev Biology - Animal* **2009**, *45*, 523.

# 국문 초록

정밀의학(Precision Medicine) 혹은 개인맞춤의학(Personalized Medicine)은 개개인의 최적화된 치료방법을 결정하는 것을 목표로 하는 의학의 패러다임이다. 특히, 임상종양학에서는 차세대염기서열분석(NGS), 전사체서열분석, 그리고 질량분석법들을 통한 환자의 분자 프로파일(molecular profile) 방법이 발전해오고 있으며, 이를 바탕으로 환자를 세분화하여 맞춤형 치료를 구현하려고 노력해오고 있다. 하지만, 여전히 현 수준에서 이해되지 못하는 수준의 종양 이질성(tumor heterogeneity)과 오랜 처방기록을 가진 환자군들의 항암제 획득 내성(acquired resistance) 등의 원인으로 맞춤형 환자 처방은 쉽지 않은 경우가 많다. 이러한 경우 환자로부터 얻어진 암세포, 조직으로부터 얻어진 일차세포 혹은 체외 배양된 세포, 스페로이드, 장기유사체 등을 이용하여 고속다중약물스크리닝기술을 통한 맞춤형 항암제를 선별해내는 체외 약물진단 기술을 생각해낼 수 있는데, 이는 기존의 유전체 기반의 시도와 병행되어 개개의 환자들에게 더욱 적합한 치료방법을 찾는 것이 가능하게 한다.

하지만 이러한 목적의 고속다중약물스크리닝기술은 높은 활용가능성에도 불구하고, 광범위한 보급과 활용이 되기에는 제약점이

많았다. 기존의 고속다중약물스크리닝기술은 많은 양의 샘플이 소모되고, 값비싼 시약의 소모량도 적지 않았다. 게다가, 수천 가지 이상의 서로 다른 물질들을 탐색하기 위해 반드시 필요한 고가의 자동화된 액체 운반기(liquid handler) 등이 필요하였는데, 이러한 문제로 대형 제약사, 연구소 등을 제외하고는 도입이 쉽지가 않아 기술접근성이 제한되어 있었다.

본 연구에서는 반도체공정에서의 노광기술을 이용하여 개개의 식별할 수 있는 코드를 가지고 있는 코드화된 하이드로젤 기반의 광경화성폴리머 미세입자를 만들어, 이를 원하는 암세포에 약물 스크리닝을 해보고자 하는 다양한 약물라이브러리를 이용 각각의 코드화된 미세입자에 흡수시켜 약물-미세입자 라이브러리를 제작한다. 그후, 값비싼 어레이 제작용 스포터 혹은 디스펜서 장비없이 간단한 자기조립을 통해 대규모의 다양한 약물-하이드로젤 어레이를 제작할 수 있는 기술을 개발하였다. 또한, 소량의 세포들 만으로도 미세우물(microwell) 기반의 세포칩에 도포하는 방식을 개발하였으며, 이를 통해 약물-하이드로젤 어레이와 미세우물기반의 세포칩의 결합으로 수백-수천의 다양한 어세이를 적은 수의 샘플만으로도 한번에 수행할 수 있는 고속다중약물스크리닝 기술을 수행할 수 있게 만들었다.

구현된 기술을 통해서 일반적으로 표적 치료제가 없어 치료가 힘든 것으로 알려진 triple negative breast cancer (TNBC) 세포를 대상으로 항암제

순차조합 스크리닝을 진행하였으며, EGFR 억제제계열의 약과 genotoxin 계열의 약물의 라이브러리를 구축하여 스크리닝을 실시한 결과 가장 좋은 효과를 나타낸 조합을 스크리닝 한 결과를 분석하였다. 또한, 실제 다점 내성을 획득한 비소세포폐암 환자의 종양으로부터 유래한 확립된 환자유래세포(Patient-Derived Cell)을 가지고 약물조합스크리닝을 통해 적합한 약물조합을 추출해보는 연구를 진행하였다. 마지막으로, 최근 실제 체내의 약물반응과 유사한 스페로이드, 장기유사체와 같은 삼차원 배양의 필요성이 더욱 증대됨에 따라, 이를 구현할 수 있는 약물스크리닝이 가능한 미세유체기반의 세포칩을 구현하는 내용 또한 개발하였다.

본 연구에서 제시한 소형화된 체외 항암제 스크리닝용 약물플랫폼은 다음과 같은 의의를 가진다. 적은 수의 환자세포 혹은 샘플의 양에 적용할 수 있는, 사용하기 손쉬운 기술로서, 기존의 값비싼 장비, 시약의 사용량을 획기적으로 줄일 수 있는 기술이다. 본 연구에서 제안된 기술을 통해 기존의 장비를 사용할 때 시약의 값이 비싸거나, 장비의 가격이 비싸서, 혹은 다루고자 하는 샘플의 양이 제한적이어서 기존에 접근하기 힘들었던 다양한 학술연구에 적용할 수 있으며, 병원에서의 임상연구 및 실제 환자맞춤형 치료에 사용 될 수 있는 접근성을 획기적으로 높일 수 있다. 특히, 비교적 중,소 규모의 연구환경에서도 다양한 희귀한 환자유래세포 혹은 환자유래오가노이드 등과 접목하여

사용된다면 본 플랫폼의 가능성을 더욱 극대화 할 수 있을 것으로 기대한다.

**주요어 :** 정밀의학, 마이크로어레이, 고속다중스크리닝, 약물조합, 코드화된 미세입자, 바이오칩

**학번 :** 2014-21752